3-1-2000

Acoustic Mechanisms that Determine the Ear-Canal Sound Pressures Generated by Earphones

Susan E. Voss
Massachusetts Eye and Ear Infirmary, svoss@smith.edu

John J. Rosowski
Massachusetts Eye and Ear Infirmary

Christopher A. Shera
Massachusetts Eye and Ear Infirmary

William T. Peake
Massachusetts Eye and Ear Infirmary

Acoustic mechanisms that determine the ear-canal sound pressures generated by earphones

Susan E. Voss
Eaton-Peabody Laboratory, Massachusetts Eye and Ear Infirmary, 243 Charles Street, Boston, Massachusetts 02114, Speech and Hearing Sciences Program, Harvard–M.I.T. Division of Health Sciences and Technology, Cambridge, Massachusetts 02139, Research Laboratory of Electronics, Massachusetts Institute of Technology, Cambridge, Massachusetts 02139, and Department of Otolaryngology, Massachusetts Eye and Ear Infirmary, 243 Charles Street, Boston, Massachusetts 02114

John J. Rosowski
Eaton-Peabody Laboratory, Massachusetts Eye and Ear Infirmary, 243 Charles Street, Boston, Massachusetts 02114, Department of Otolaryngology, Massachusetts Eye and Ear Infirmary, 243 Charles Street, Boston, Massachusetts 02114, and Department of Otology and Laryngology, Harvard Medical School, Speech and Hearing Sciences Program, Harvard–M.I.T. Division of Health Sciences and Technology, Cambridge, Massachusetts 02139

Christopher A. Shera
Eaton-Peabody Laboratory, Massachusetts Eye and Ear Infirmary, 243 Charles Street, Boston, Massachusetts 02114, Department of Otolaryngology, Massachusetts Eye and Ear Infirmary, 243 Charles Street, Boston, Massachusetts 02114, and Department of Otology and Laryngology, Harvard Medical School

William T. Peake
Eaton-Peabody Laboratory, Massachusetts Eye and Ear Infirmary, 243 Charles Street, Boston, Massachusetts 02114, Department of Electrical Engineering and Computer Science, Massachusetts Institute of Technology, 77 Massachusetts Avenue, Cambridge, Massachusetts 02139, Research Laboratory of Electronics, Massachusetts Institute of Technology, Cambridge, Massachusetts 02139, and Speech and Hearing Sciences Program, Harvard–M.I.T. Division of Health Sciences and Technology, Cambridge, Massachusetts 02139

(Received 4 August 1999, accepted for publication 3 December 1999)

In clinical measurements of hearing sensitivity, a given earphone is assumed to produce essentially the same sound-pressure level in all ears. However, recent measurements [Voss *et al.*, Ear and Hearing (in press)] show that with some middle-ear pathologies, ear-canal sound pressures can deviate by as much as 35 dB from the normal-ear value; the deviations depend on the earphone, the middle-ear pathology, and frequency. These pressure variations cause errors in the results of hearing tests. Models developed here identify acoustic mechanisms that cause pressure variations in certain pathological conditions. The models combine measurement-based Thévenin equivalents for insert and supra-aural earphones with lumped-element models for both the normal ear and ears with pathologies that alter the ear's impedance (mastoid bowl, tympanostomy tube, tympanic-membrane perforation, and a ''high-impedance'' ear). Comparison of the earphones' Thévenin impedances to the ear's input impedance with these middle-ear conditions shows that neither class of earphone acts as an ideal pressure source; with some middle-ear pathologies, the ear's input impedance deviates substantially from normal and thereby causes abnormal ear-canal pressure levels. In general, for the three conditions that make the ear's impedance magnitude lower than normal, the model predicts a reduced ear-canal pressure (as much as 35 dB), with a greater pressure reduction with an insert earphone than with a supra-aural earphone. In contrast, the model predicts that ear-canal pressure levels increase only a few dB when the ear has an increased impedance magnitude; the compliance of the air–space between the tympanic membrane and the earphone determines an upper limit on the effect of the middle-ear's impedance increase. Acoustic leaks at the earphone-to-ear connection can also cause uncontrolled pressure variations during hearing tests. From measurements at the supra-aural earphone-to-ear connection, we conclude that it is unusual for the connection between the earphone cushion and the pinna to seal effectively for frequencies below 250 Hz. The models developed here explain the measured pressure variations with several pathologic ears. Understanding these mechanisms should inform the design of more accurate audiometric systems which might include a microphone that monitors the ear-canal pressure and corrects deviations from normal. [S0001-4966(00)03403-2]

PACS numbers: 43.64.Yp, 43.64.Bt [BLM]

INTRODUCTION

A. A basic problem in audiometric testing

A common clinical test of hearing sensitivity is the pure-tone ''audiogram'' in which the lowest sound-pressure level at which the subject can hear a tone is determined at several frequencies. For the testing, a loudspeaker may generate a sound field around the subject, but more typically an earphone is coupled to the subject's ear; in either case, the subject indicates whether or not the sound is perceived so as to determine the hearing ''threshold'' versus frequency, i.e., the ''audiogram.'' In this study we focus on the acoustic response in the ear canal with two earphone configurations, namely an insert and a supra-aural earphone.

Ear-canal sound-pressure levels during audiometric tests are not generally measured. Instead, the level of the sound stimulus is determined by the setting of an attenuator that controls the electric input to the sound source, and it is assumed that the earphone's calibration (sound-pressure output per volt input) is independent of variation in the acoustic properties of individual ears (e.g., Burkhard and Corliss, 1954; Shaw, 1974; Kruger and Tonndorf, 1977, 1978; Borton *et al.*, 1989; Wilber, 1994). In other words, it is assumed that an earphone's sound-pressure output is not greatly affected by the impedance of the ear to which it is coupled. However, measurements with two earphone configurations (insert and supra aural) of the pressures generated in ear canals of pathologic middle ears show pressure levels that differ from normal by as much as 35 dB (Voss *et al.*, in press). These variations introduce errors of the same size in the measurement of audiograms.

The pressure generated by an earphone can also be affected by acoustic leaks between the earphone and the ear. As Zwislocki *et al.* (1988) write, ''Supra-aural earphones have low reliability at low frequencies because of variable and unstable coupling between the earphone and the ear. Air leaks occurring between the earphone cushion and the pinna produce variable amounts of sound-pressure loss at low frequencies (typically below 500 Hz), accompanied by small, variable amounts of sound-pressure enhancement at somewhat higher frequencies (between 500 and 1000 Hz).''

The theory presented here investigates the acoustic mechanisms that affect the ear-canal pressure level generated by two types of audiologic earphones, an insert earphone and a supra-aural earphone. We combine measurements of the Thévenin equivalents for the earphones with models for (a) the ear canal, (b) the normal middle ear, (c) the middle ear with specific pathologies, and (d) leaks in the earphone-ear connection, and we use these models to predict how these different conditions affect the ear-canal pressures generated by the earphones. We compare these predictions to our recent measurements (Voss *et al.*, in press).

B. Ear impedance and middle-ear pathology

Some middle-ear pathologies have been shown to alter the ear's input impedance (e.g., Zwislocki, 1962; Zwislocki and Feldman, 1970); other pathologies can also be expected to cause large changes in the ear's impedance. For example, tympanic-membrane perforations[1] provide a direct connection between the ear canal and the middle-ear air space [Fig. 1(B)], which reduces the impedance at the tympanic membrane for low frequencies (Voss, 1998). Similarly, tympanostomy tubes,[2] which are inserted through the tympanic membrane to manage middle-ear disease [Fig. 1(C)], also reduce the low-frequency impedance of the middle ear via the same mechanism. Our third pathological configuration, ''mastoid bowl,'' results from ''canal-wall down'' mastoid surgery (see, e.g., Nadol, 1993, pp. 104–106). This procedure, which is performed to remove middle-ear disease, opens the mastoid portion of the middle-ear air spaces and externalizes this space by connecting it to the ear canal by removal of a portion of the posterior and superior bony-canal

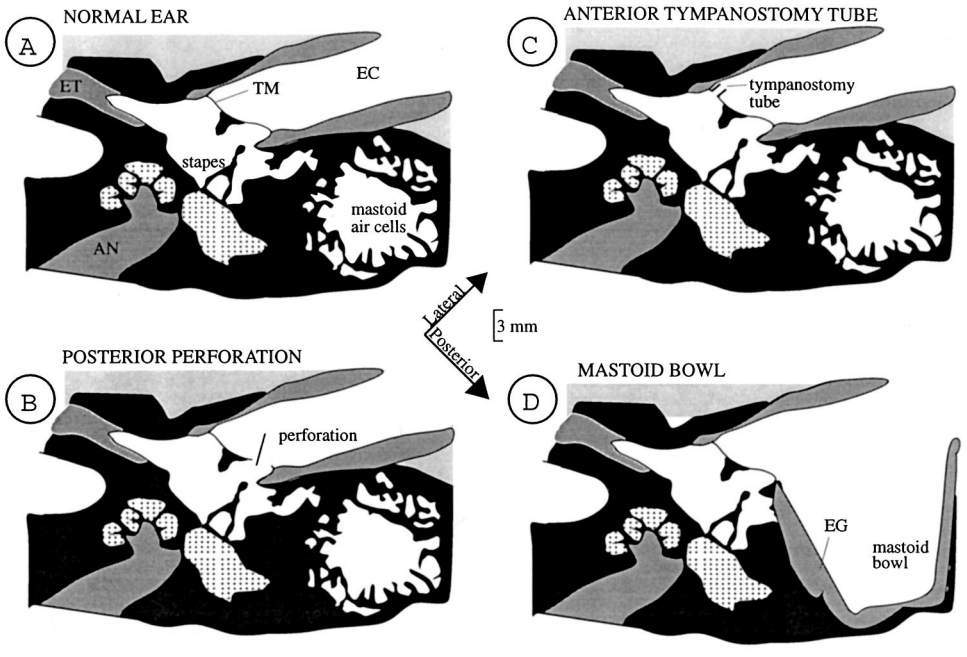

FIG. 1. Structural modifications in three middle-ear pathologies. All four figures portray a horizontal section through the middle ear at the level of the stapes. Bone is black, fluid is dotted, air is white, and soft tissue is gray. (ET=Eustachian tube; AN=auditory nerve; EC=ear canal; TM=tympanic membrane.) (A) Normal ear. (B) Perforation of the tympanic membrane. (C) Tympanostomy tube in the tympanic membrane. (D) Mastoid-bowl cavity connecting to the ear canal. (EG =Epithelial graft.)

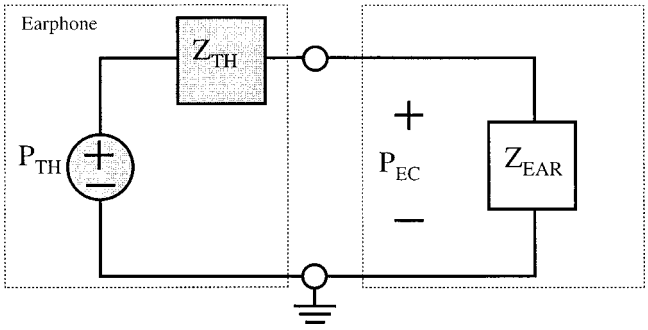

FIG. 2. Electric-circuit analog that represents acoustic variables for an earphone coupled to an ear. The earphone is represented by its Thévenin equivalent (shaded gray): a pressure source P_{TH} and an impedance Z_{TH}. Z_{EAR}, the acoustic load on the earphone, is represented by the white block. P_{EC} is the pressure generated by the earphone in the ear canal. The labeled quantities are acoustic quantities with sound pressure analogous to voltage relative to ''ground'' and volume velocity analogous to current (i.e., the ''impedance analogy'').

wall. The resulting ''mastoid bowl'' introduces a 1 to 6 cm^3 air volume to the external ear (Merchant, 1997) [Fig. 1(D)].

Other middle-ear pathologies have been shown to increase the ear's impedance magnitude relative to normal. Abnormal growth in the petrous bone can reduce movement of the stapes in otosclerosis (Zwislocki and Feldman, 1970), and fluid in the middle-ear cavity can impede tympanic membrane and ossicular motion in otitis media (Berry *et al.*, 1975).

The goal of this paper is to understand the mechanisms through which such pathologies alter sound pressures generated in the ear canal by insert and supra-aural earphones.

C. Theory

Audiometric practice assumes that the ear-canal pressure P_{EC} is nearly independent of the ear to which the earphone is coupled. In this section we examine the constraints that make this assumption accurate.

In the analog-circuit model of Fig. 2, P_{EC} can be expressed in terms of the earphone's Thévenin parameters, P_{TH} and Z_{TH}, and the ear's impedance, Z_{EAR}:

$$\frac{P_{EC}}{P_{TH}} = \frac{1}{1+Z_{TH}/Z_{\mathrm{EAR}}}, \tag{1}$$

where P_{TH} is proportional to the input voltage applied to the earphone. The ratio between the ear-canal pressure generated in a test ear and the pressure generated in an average normal ear can be expressed in terms of $\Delta Z \equiv Z_{\mathrm{EAR}} - Z_{\mathrm{EAR}}^{\mathrm{NORMAL}}$ as

$$\frac{P_{EC}}{P_{EC}^{\mathrm{NORMAL}}} = 1 + \frac{\Delta Z_{\mathrm{EAR}}/Z_{\mathrm{EAR}}^{\mathrm{NORMAL}}}{1+Z_{\mathrm{EAR}}/Z_{TH}}, \tag{2}$$

where $Z_{\mathrm{EAR}}^{\mathrm{NORMAL}}$ is the impedance of an average normal ear and Z_{EAR} is the impedance of the test ear. Thus, for $|P_{EC}/P_{EC}^{\mathrm{NORMAL}}|$ to be approximately one, the term $(\Delta Z_{\mathrm{EAR}}/Z_{\mathrm{EAR}}^{\mathrm{NORMAL}})/(1+Z_{\mathrm{EAR}}/Z_{TH})$ in Eq. (2) must have a magnitude that is much less than one. If $|Z_{\mathrm{EAR}}/Z_{TH}| \to \infty$, so that the earphone acts as an ideal pressure source, the approximation would hold for any finite $|\Delta Z_{\mathrm{EAR}}|$. However, our measurements show that typical earphones do not approximate pressure sources, but rather $0.9 < |1+Z_{\mathrm{EAR}}/Z_{TH}| < 3$.

Consequently, to satisfy the assumption that P_{EC} is nearly independent of Z_{EAR}, impedance variations among ears, ΔZ_{EAR}, must be small relative to $Z_{\mathrm{EAR}}^{\mathrm{NORMAL}}$. We show here that this constraint is also violated for some middle-ear pathologies. For example, using the ER-3A insert earphone in an ear with a 4-cm^3 mastoid bowl at 1000 Hz, $\Delta Z_{\mathrm{EAR}}/Z_{\mathrm{EAR}}^{\mathrm{NORMAL}} \approx -0.8$, so that (with $1+Z_{\mathrm{EAR}}/Z_{TH} \approx 1$) $|P_{EC}/P_{EC}^{\mathrm{NORMAL}}| \approx 0.2$, and the sound pressure in the ear is about -14 dB relative to the assumed calibration value, which leads to an overestimate of hearing loss by about 14 dB.

I. THÉVENIN EQUIVALENTS FOR EARPHONES

A. Measurement methods

An insert earphone (Etymōtic ER-3A) and a supra-aural earphone (TDH-49 with an MX-41/AR cushion) were each modified to include a microphone (Voss *et al.*, in press and Fig. 3). The insert earphone was coupled to the standard yellow-foam ear plug (Earlink™; uncompressed diameter 14 mm, length 12 mm), and a flexible probe tube (Etymōtic Research ER7-14C) was threaded through the foam plug. One end of the probe tube extended 3 mm beyond the medial end of the plug, and the other end was coupled to the microphone. With the supra-aural earphone, a steel tube was inserted through the earphone's cushion so that one end was at the earphone's output port and the other end exited along the cushion's outer circumference. A flexible probe tube (Etymōtic Research ER7-14C) was placed through the steel tube; the inner end of the probe tube was less than 1-mm lateral to the earphone port and the other end coupled to the microphone. The flexible probe fit snugly in the steel tube.

The Thévenin equivalents were determined for each earphone from pressure measurements in two ''reference loads'' of theoretically known impedance (see, e.g., Rabinowitz, 1981; Allen, 1986; Lynch *et al.*, 1994). The reference loads were a short closed cavity and a long open tube, which are described further in Fig. 3.

The pressure measurements were made using an Ariel DSP-16+ board with SYSid™ software (e.g., Voss and Allen, 1994). The software reports the Fourier transform of the sampled and averaged time-domain response. The responses to chirp stimuli were sampled at 50 kHz and averaged over 200 repetitions. The DFT length was 2048 points for all measurements except those made in the long open tube that attached to the supra-aural earphone [Fig. 3(D)], which had a DFT length of 8192 points.

The impulse response computed from the pressure measurement made in the long open tube attached to the supra-aural earphone showed energy that was delayed by more than 10 ms in time relative to the electric stimulus. This energy appeared to result from reflections in the tube at locations remote to the earphone. Because such reflections are not included in the uniform tube model that is used for the theoretical impedance of the long tube, to remove their effects we set the impulse response to zero for all times greater

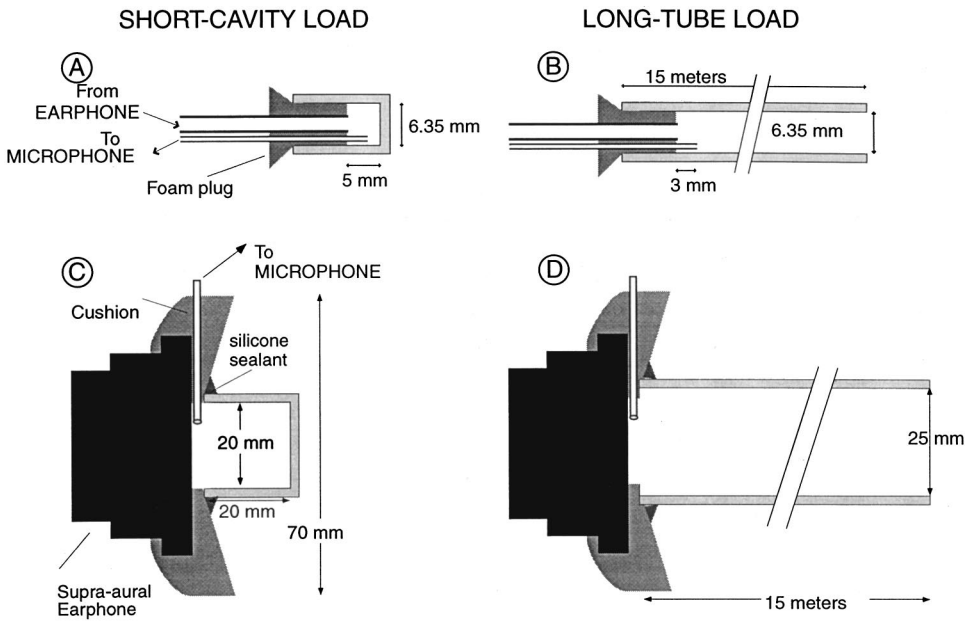

FIG. 3. Schematic showing how the insert [(A) and (B)] and the supra-aural [(C) and (D)] earphones were coupled to the microphone-probe tube and to the calibration loads. (A) The insert earphone coupled to the short closed tube with a rigid termination, inner diameter i.d.=6.35 mm and length $l=2$ mm from the microphone's probe tube. (B) The insert earphone coupled to the long tube with an open termination with i.d.=6.35 mm and length $l=15$ m. (C) The supra-aural earphone coupled to the short closed tube with a rigid termination, i.d.=20 mm and length $l=20$ mm. (D) The supra-aural earphone coupled to the tube with an open termination, i.d.=25 mm and length $l=15$ m.

than 10 ms and used the DFT of this signal as the pressure frequency response.

The theoretical impedances of all reference loads were calculated from the equations of Egolf (1977). For each earphone, the pressure measurements made in the two loads were combined with the loads' theoretical impedances to calculate the Thévenin pressure source and impedance: P_{TH}^{I} and Z_{TH}^{L} for the insert earphone and P_{TH}^{SA} and Z_{TH}^{SA} for the supra-aural earphone.

B. Results: Thévenin equivalents

Our measurements of the Thévenin pressures and impedances for both insert and supra-aural earphones are shown in Fig. 4. The Thévenin acoustic output impedances are nearly identical for the two (ER-3A) insert earphones, where ''Earphone A'' has an electric input impedance of 50 Ω and ''Earphone B'' has an electric input impedance of 10 Ω, and the two Thévenin pressures differ by about 5 dB at most frequencies. The Thévenin impedance magnitude of the supra-aural earphone is about one tenth that of the insert earphones.

These descriptions of the earphones are used in Sec. III to predict the pressure that the earphones generate in ear canals.

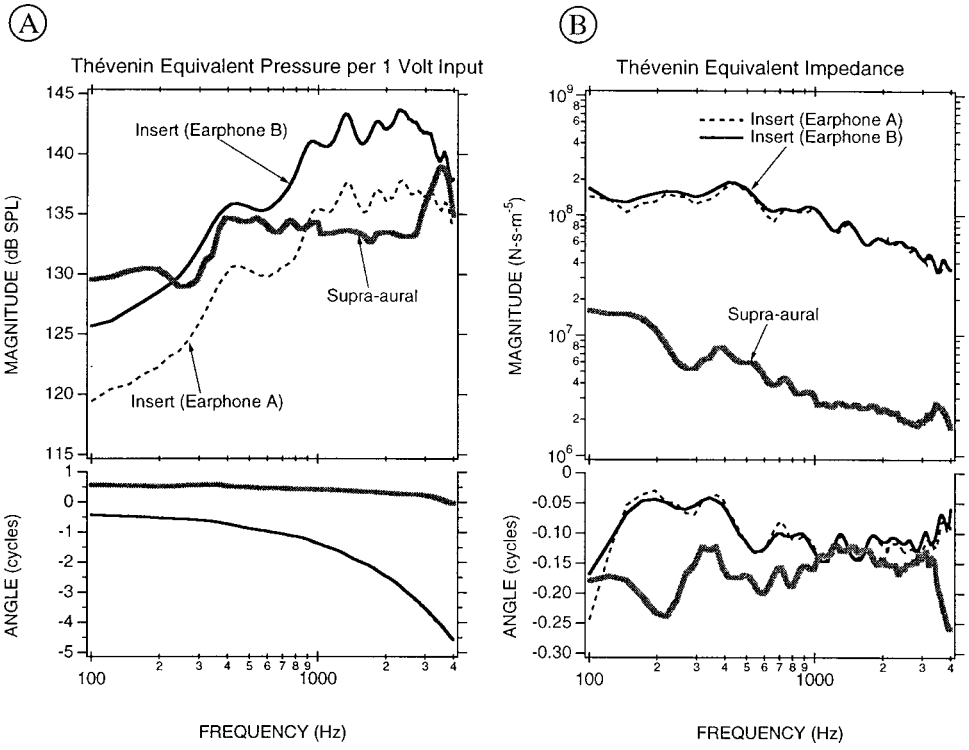

FIG. 4. Thévenin equivalents for the insert earphone and the supra-aural earphone. (A) Thévenin pressures. (B) Thévenin impedances. UPPER: Magnitudes. LOWER: Angles. The Thévenin pressure angles for the insert earphones correspond to a constant delay of about 1.1 ms—the time it takes sound to travel about 35 cm—which is the length of plastic tubing through which sound generated by the insert earphone must travel. Earphone A is an ER-3A insert earphone with a nominal input impedance of 50 Ω and earphone B is an ER-3A with an input impedance of 10 Ω. The angles of the equivalent pressure of the two insert earphones are essentially identical.

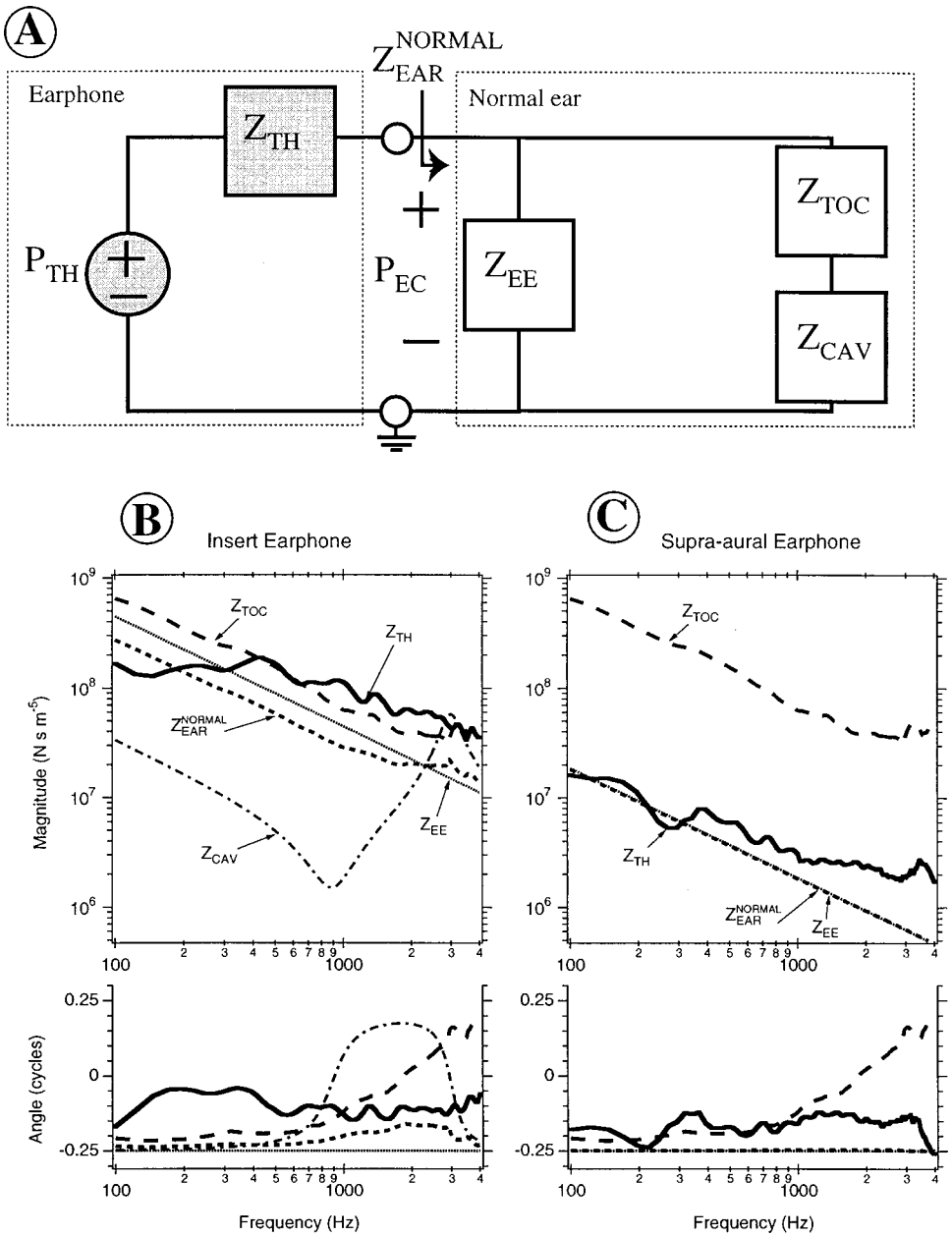

FIG. 5. (A) Lumped-element model for the normal middle ear connected to an earphone represented by its Thévenin equivalent circuit P_{TH} and Z_{TH} (shaded gray). $Z_{\mathrm{EAR}}^{\mathrm{NORMAL}}$, the driving-point impedance of the ear, is the load driven by the earphone. Z_{EE} represents the external-ear air space between the tympanic membrane and the earphone as a compliance corresponding to $V_{EE}^{I}=0.5\ \mathrm{cm}^3$ and $V_{EE}^{SA}=12.0\ \mathrm{cm}^3$ for the insert and the supra-aural earphones, respectively. Z_{TOC} represents the tympanic membrane (T), ossicular chain (O), and cochlea (C), and the values used for Z_{TOC} are means from measurements in normal temporal bones ($N=9$) (Voss, 1998), which are comparable to the measurements of Rosowski *et al.* (1990). The standard deviation for $|Z_{\mathrm{TOC}}|$ is less than 6 dB at all frequencies, and the standard deviation for $\angle Z_{\mathrm{TOC}}$ is less than 0.05 cycles below 1000 Hz and less than 0.10 cycles above 1000 Hz. Z_{CAV} represents an average middle-ear cavity and is defined in Fig. 6. (B) Impedance magnitudes and angles with the insert earphone. (C) Impedance magnitudes and angles with the supra-aural earphone.

II. MODELS FOR EARS COUPLED TO EARPHONES

A. Goals and approach

We propose simple circuit models to represent two earphone configurations (i.e., insert and supra-aural) coupled to a normal ear, coupled to four types of pathologic ears, and incorporating acoustic leaks between the supra-aural earphone and the ear. Our goal is to use these models to test our understanding of the acoustic mechanisms that are important in determining the ear-canal sound pressure generated under these different conditions. In the next section (Sec. III) we use these models to make predictions for the ear-canal sound pressure in each of the configurations.

We plot our model predictions for a frequency range of 100–4000 Hz, which contains the important audiologic frequencies. The lumped-element analog model is accurate only when the dimensions of the ear canal and ear are small relative to the wavelength of sound. With the insert earphone and a normal ear, the largest dimension is the ear-canal length of about 13 mm, which is 15% of the 88-mm wavelength of sound at 4000 Hz; thus, the lumped model should accurately represent the acoustic variations for frequencies up to 4000 Hz. With the supra-aural earphone and a normal ear, the largest dimension of the ear is much larger than with the insert earphone: the ear-canal length plus the distance from the ear canal to the earphone is about 50 mm. Here, the frequency at which the largest dimension is 15% of a wavelength is only 1050 Hz. Thus, with the supra-aural earphone the lumped model becomes inaccurate at lower frequencies than with the insert earphone.

B. The normal ear

The lumped-element model for the normal middle ear [Fig. 5(A)] consists of three impedances. Z_{EE} represents the external-ear (EE) air space between the tympanic membrane

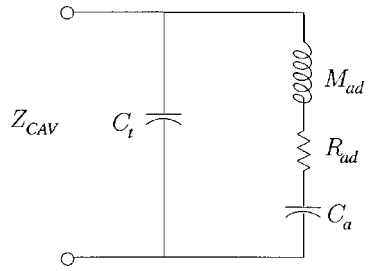

FIG. 6. Lumped-element model that represents the middle-ear cavity impedance Z_{CAV} (Voss, 1998). Element values determined by Voss (1998) from measurements of Z_{CAV} made on temporal bones are: $C_t = 4.2\times10^{-12}$ F, where C_t has an equivalent volume V_t of 0.6 cm^3; $M_{ad} = 722$ H; $R_{ad} = 0.05\times10^6\sqrt{f}\,\Omega$, where f is frequency (in Hz); and $C_a = V_a/(\rho c^2)$, where V_a is the volume of the antrum and other mastoid air cells. Here, unless noted otherwise, $V_a = 5.9$ cm^3 ($C_a = 42\times10^{-12}$ F), which when added to the tympanic-cavity volume of 0.6 cm^3, results in the total middle-ear cavity volume of 6.5 cm^3 as measured (average) by Molvaer *et al.* (1978). In cases where the middle-ear cavity volume is varied, the tympanic-cavity volume remains constant at 0.6 cm^3, and the volume of the antrum and other mastoid air cells, V_a, is varied.

and the earphone and is modeled as a compliance [i.e., $Z_{EE} = 1/(j\omega C_{EE})$] with a value appropriate for the external-ear air space (i.e., $C_{EE} = V_{EE}/(\rho c^2)$, where ρ is the density of air, c is the speed of sound in air, and V_{EE} is the external-ear air volume). External-ear air volumes for the insert earphone and the supra-aural earphone are selected as $V_{EE}^{I} = 0.5$ cm^3 and $V_{EE}^{SA} = 12.0$ cm^3 respectively.[3] [Z_{EE} is plotted in Fig. 5(B) and (C) for both cases.] The impedance that represents the external-ear air volume is assumed constant for all middle-ear conditions and is placed in parallel with the impedances that represent the middle ear to represent the portion of the volume velocity generated by the earphone that compresses the air in the external-ear; the rest of the volume velocity represents movement of the tympanic membrane. We will see that the external-ear volume plays an important role in the ear's impedance; the difference between the insert earphone's smaller external-ear volume and the supra-aural earphone's larger external-ear volume is partially responsible for earphone-linked differences in the effects of altered middle-ear impedances on ear-canal pressures.

Our lumped-element model represents the middle ear by two impedances in series: Z_{TOC} and Z_{CAV}. Z_{TOC} represents the tympanic membrane (T), ossicular chain (O), and cochlea (C), and the Z_{TOC} we use [see Fig. 5(B) and (C)] is the mean from temporal-bone measurements (Voss, 1998; Fig. 4-2). Z_{CAV} represents the middle-ear cavity. The model we use for Z_{CAV} (Fig. 6) is the same topology used in Kringlebotn's (1988) middle-ear model, but some of the element values were determined from measurements of Z_{CAV} on human temporal bones (Voss, 1998, pp. 168–173). In this model, C_t represents the compliance of the tympanic cavity, with $C_t = V_t/(\rho c^2)$, M_{ad} and R_{ad} represent the ''tubelike'' aditus ad antrum that connects the tympanic cavity and the mastoid cavity (Voss, 1998, pp. 168–169); and C_a represents the compliance of the antrum and other air cells, with $C_a = V_a/(\rho c^2)$, where V_a is the total volume of the antrum and other mastoid air cells. The impedance Z_{CAV} is plotted in Fig. 5(B).

In a normal ear, $|Z_{\mathrm{TOC}}| \gg |Z_{\mathrm{CAV}}|$ so that the ear's input impedance, $Z_{\mathrm{EAR}}^{\mathrm{NORMAL}}$, is well approximated by the parallel combination of Z_{EE} and Z_{TOC}. Since $|Z_{EE}| < |Z_{\mathrm{TOC}}|$ for both earphone configurations, Z_{EE} plays an important role in determining Z_{EAR}. The impedance values for $Z_{\mathrm{EAR}}^{\mathrm{NORMAL}}$ are plotted in Fig. 5(B) and (C). Because the external-ear volume is much larger with the supra-aural earphone than with the insert earphone, the driving-point impedance magnitude of the normal ear, $|Z_{\mathrm{EAR}}^{\mathrm{NORMAL}}|$, is much smaller with the supra-aural earphone than with the insert earphone.

Figure 5(B) and (C) allows comparison of the Thévenin-impedance magnitudes for each source to that of the normal ear. Neither Thévenin impedance meets the condition required for a nearly ideal pressure source, namely that $|Z_{TH}| \ll |Z_{\mathrm{EAR}}^{\mathrm{NORMAL}}|$ (Sec. C of the Introduction). In fact, for both earphone configurations $|Z_{TH}| > |Z_{\mathrm{EAR}}^{\mathrm{NORMAL}}|$ for frequencies above 700 Hz. Thus, for ear-canal pressures to be nearly independent of the attached ear, pathologic changes in Z_{EAR} must be small relative to the normal value for Z_{EAR}. Subsequent sections of this paper determine whether this condition is met for either earphone configuration with ears having middle-ear pathologies and earphone-ear connections with acoustic leaks.

C. Pathologic ears

1. Scope

To create models for three pathologic conditions (mastoid-bowl ear, tympanostomy-tube ear, and tympanic-membrane-perforation ear) and one condition that approximates pathological ears with ''high-impedances,'' we modify the lumped-element model for the normal ear [Fig. 5(A)] by adding elements.

2. Mastoid-bowl ear

The effect of the mastoid bowl [Fig. 1(D)] is represented by an added impedance Z_{BOWL} in parallel with the ear-canal air space and the normal middle-ear components [Fig. 7(A)]. Z_{BOWL} is a compliance, with an equivalent volume equal to the physical volume of a mastoid bowl, which can range from about 1 to 6 cm^3 (Merchant, 1997). The additional air volume acts to decrease the magnitude of the ear's driving-point impedance; the greater the bowl's volume, the more the impedance magnitude decreases relative to normal. The impedance magnitudes for the driving-point impedance of an ear with a mastoid bowl, $Z_{\mathrm{EAR}}^{\mathrm{MB}}$, with bowl volumes of 1 cm^3 and 6 cm^3 are compared to the Thévenin impedances of the two sources in Fig. 7(B) and (C).

For the insert earphone, $|Z_{\mathrm{EAR}}^{\mathrm{MB}}| < |Z_{\mathrm{EAR}}^{\mathrm{NORMAL}}|$ for both bowl volumes, and the impedance of the mastoid bowl is approximately the driving-point impedance of the ear $Z_{\mathrm{EAR}}^{\mathrm{MB}}$. Moreover, the condition that variations in Z_{EAR} must be small relative to $Z_{\mathrm{EAR}}^{\mathrm{NORMAL}}$ (Sec. C of the Introduction) is grossly violated for the insert earphone; with the larger mastoid bowl the ear's impedance magnitude $|Z_{\mathrm{EAR}}^{\mathrm{MB}}|$ decreases to about 1/7 the value for a normal ear.

The relative impedance magnitudes are somewhat different with the supra-aural earphone. In this case, the additional volume introduced by the mastoid bowl is less than the 12-cm^3 air volume between the source and the tympanic

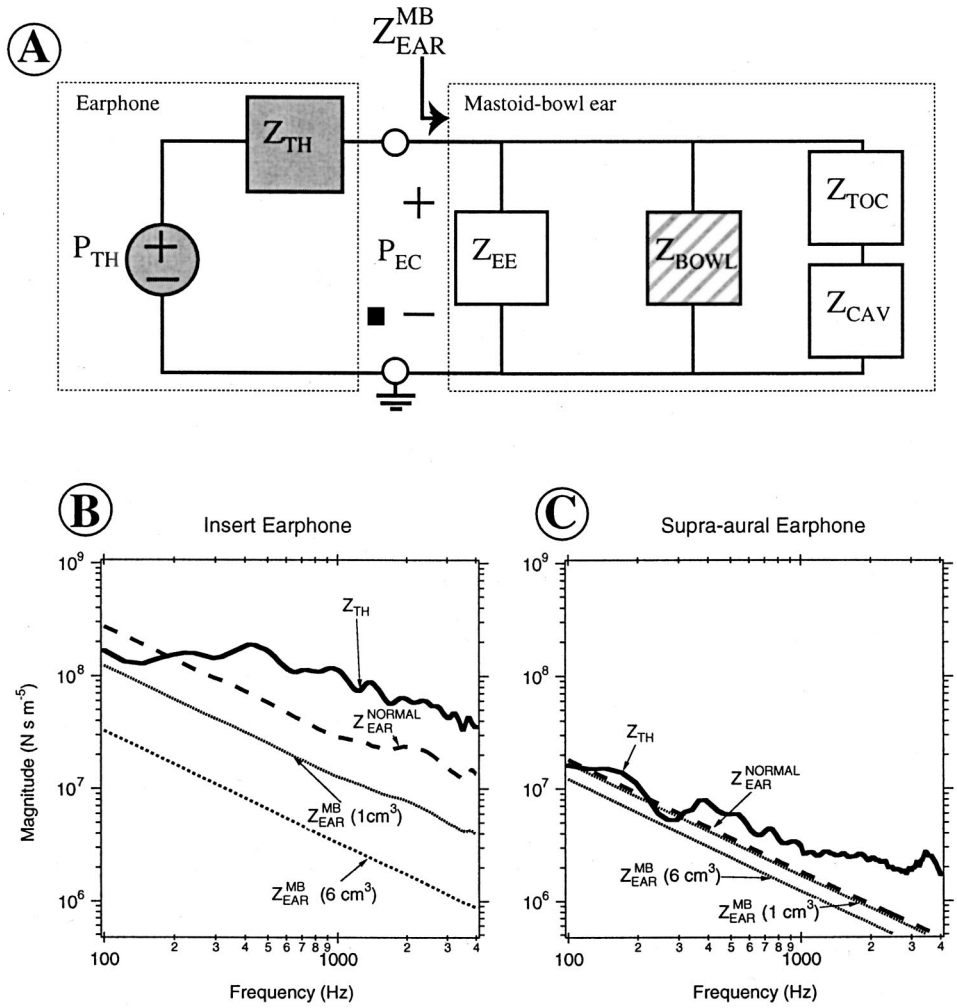

FIG. 7. (A) Lumped-element model for an earphone with Thévenin source characteristics (shaded gray) P_{TH} and Z_{TH} that is connected to an ear with a mastoid bowl (MB). The white blocks are identical to the normal middle ear of Fig. 5(A). The striped box labeled Z_{BOWL} is a compliance with an equivalent volume equal to the volume of the mastoid bowl. (B) Impedance values for the model of *A* with the insert earphone. Z_{EAR}^{MB} the driving-point impedance of the ear with a mastoid bowl (*MB*), is shown for two mastoid bowl volumes, 1 and 6 cm^3, that span the usual range. (C) Impedance values for the model of *A* with the supra-aural earphone.

membrane in the normal ear. Therefore, the effect of a mastoid bowl, though it still reduces the driving-point impedance magnitude, is much smaller with the supra-aural earphone. With a mastoid volume of 6.0 cm^3, the impedance magnitude decreases by less than a factor of 2 relative to the normal ear. Thus, the condition required for constant ear-canal pressures—that variations in Z_{EAR} must be small relative to $Z_{\mathrm{EAR}}^{\mathrm{NORMAL}}$—is more closely approximated with the supra-aural earphone.

The frequency range for which the lumped-element model is valid depends on the largest dimensions of the ear. A mastoid bowl modifies the ear canal and increases the external-ear and ear-canal dimensions relative to normal. With the insert earphone and a normal ear the largest dimension was identified as the effective ear-canal length of about 13 mm; a mastoid bowl may increase this dimension and thus reduce the upper valid frequency limit of 4000 Hz. With the supra-aural earphone, the largest dimension of about 50 mm probably does not increase much with the addition of a mastoid bowl, and the upper limit for our model probably remains at about 1000 Hz. As we will see (Sec. III C), the ''simple'' lumped-element model of Fig. 7(A) fails to capture pressure extrema that occur in the experimental data at frequencies above 1000 Hz with the supra-aural earphone. In order to increase the valid frequency range for the model of a supra-aural earphone coupled to a mastoid-bowl ear, we will represent the external ear (i.e., Z_{EE}) by several lumped elements (Sec. III E).

3. Tympanostomy-tube ear

The tympanostomy tube is modeled as a lossy tube, with impedance Z_{TUBE}, connecting the ear-canal air space to the middle-ear cavity space [Fig. 8(A)]; the volume velocity through Z_{TUBE} contributes to the volume velocity into Z_{CAV}.

The impedance Z_{TUBE} is calculated from the lossy equations of Egolf (1977), with the length of the tube $l = 2.1$ mm and the diameter $d = 1.27$ mm corresponding to the dimensions of a Baxter™ tympanostomy tube. To compute Z_{TUBE}, we reduce Egolf's two-port network model of a tube to a one-port element by computing the input impedance of the two-port network terminated with an impedance of zero. Z_{TUBE} is approximately a mass in series with a small resistance [$|Z_{\mathrm{TUBE}}|$ as plotted in Fig. 8(B)].

The impedance magnitudes for an ear with a tympanostomy tube $Z_{\mathrm{EAR}}^{\mathrm{TUBE}}$ are plotted for both earphone configurations [Fig. 8(B) and (C)]. Here, because of the tube's connection to it, the middle-ear cavity impedance Z_{CAV} becomes an important element in the model. At the lowest frequency plotted (100 Hz), $|Z_{\mathrm{TUBE}}| \ll |Z_{\mathrm{TOC}}|$ and $|Z_{\mathrm{TUBE}}| \ll |Z_{\mathrm{CAV}}|$, independent of earphone configuration; thus, the driving-point impedance Z_{EAR} is essentially the parallel combination of

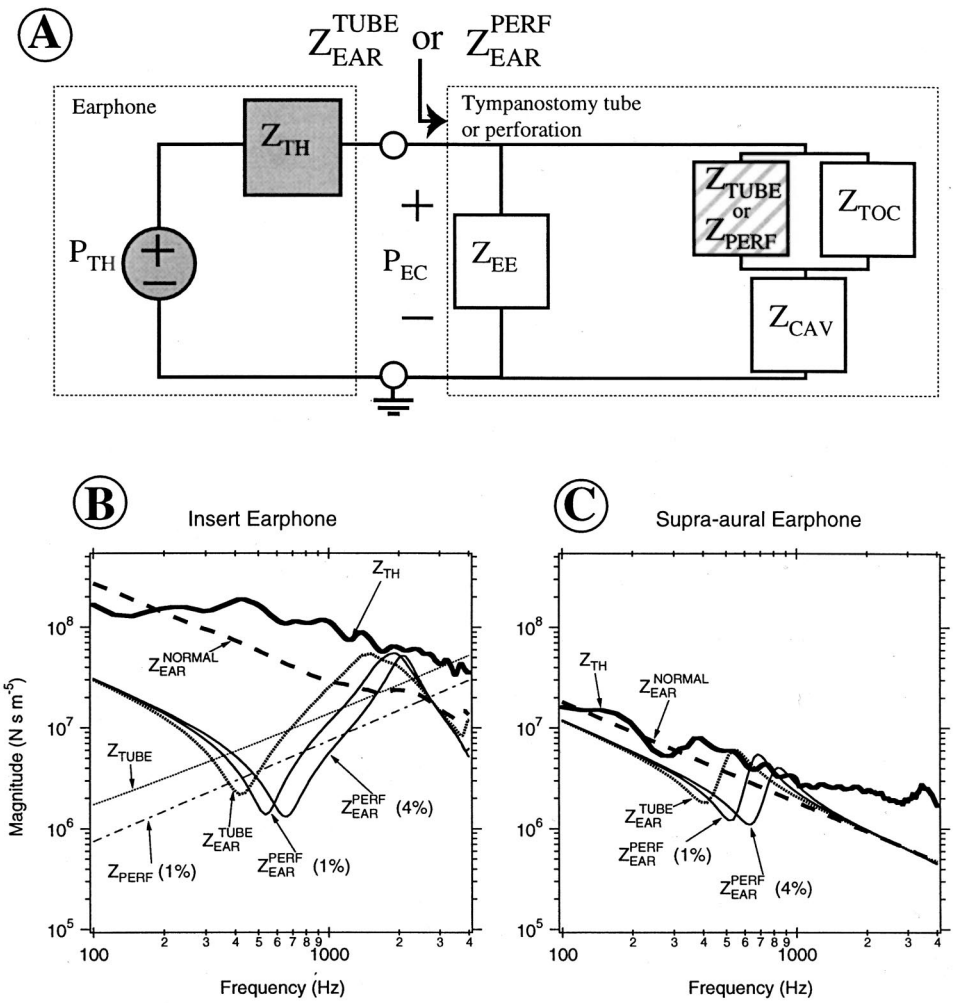

FIG. 8. (A) Model for ears with either a tympanostomy tube (TUBE) or tympanic-membrane perforation (PERF). Z_{EAR}^{TUBE} is the driving-point impedance of the ear with a tympanostomy tube, and Z_{EAR}^{PERF} is the driving point impedance of the ear with a perforation, where the percent of tympanic-membrane area covered by the perforation is indicated. The white blocks are identical to the normal middle ear of Fig. 5(A). The box with stripes is an approximation for a lossy tube that represents a tympanostomy tube (Z_{TUBE}) or a circular orifice with negligible thickness that represents a tympanic-membrane perforation (Z_{PERF}) (see text for details). (B) Impedance values for the model with the insert earphone. (C) Impedance values with the supra-aural earphone.

two compliance-dominated impedances, Z_{EE} and Z_{CAV}. As frequency increases, Z_{TOC} remains relatively unimportant; Z_{TUBE}, which can be approximated by an acoustic mass, M_{TUBE}, increases in magnitude; and a series resonance between the acoustic mass of the tube and the ''effective'' compliance of the middle-ear cavity[4] occurs between 300 and 400 Hz. This resonance results in an impedance-magnitude minimum at frequency f_{min}, which depends on the dimensions of the tympanostomy tube and the middle-ear cavity volume and is independent of the type of earphone (i.e., insert or supra-aural). The depth of the impedance minimum does depend on the earphone type because the driving-point impedance Z_{EAR} depends on Z_{EE}, which changes with earphone type. As frequency increases further, a peak at frequency f_{max} occurs as a result of a parallel resonance between the compliance of the external-ear volume and the effective middle-ear cavity compliance and the mass of the tube. The frequency f_{max} depends on the external-ear volume and is thus different for the two earphones.

Large variations of Z_{EAR}^{TUBE} relative to Z_{EAR}^{NORMAL} occur in ears with tubes [Fig. 8(B) and (C)]. The magnitude variations are larger for the insert earphone than for the supra-aural earphone, but the supra-aural earphone variations can be substantial near the resonant frequencies. Thus, the condition (Sec. C of the Introduction) required for constant ear-canal pressures—that variations in Z_{EAR} must be small relative to Z_{EAR}^{NORMAL}—is not met at some lower frequencies for ears with tympanostomy tubes.

4. Tympanic-membrane perforations

The model for a tympanic-membrane perforation is identical in topology to the tympanostomy tube; the perforation's impedance Z_{PERF} is placed between the external-ear volume and the middle-ear cavity, and the impedance Z_{PERF} is calculated using equations from Morse and Ingard (1968, pp. 480–483) for a circular orifice with negligible thickness, where $Z_{PERF}=j\omega M_{PERF}+R_{PERF}$ is the series combination of $M_{PERF}=\rho/d$ with ρ the density of air and d the perforation's diameter, and $R_{PERF}=1/[4\pi(d/2)^2]\sqrt{2\rho\omega\mu}\ln(d/h)$ with h the larger of two quantities: (1) half the thickness of the tympanic membrane, where the thickness of the tympanic membrane equals 0.1 mm (Lim, 1970), or (2) the thickness of the viscous boundary layer $d_v=\sqrt{2\mu/(\rho\omega)}$, where μ is the absolute viscosity of air. The calculated $|Z_{PERF}|$ with a 1-mm-diameter perforation is included in Fig. 8(B).

Impedance magnitudes for the ear with two different sized tympanic-membrane perforations Z_{EAR}^{PERF} (covering 1% and 4% of the tympanic-membrane area[5]) are plotted for both earphones [Fig. 8(B) and (C)]. The impedance's behav-

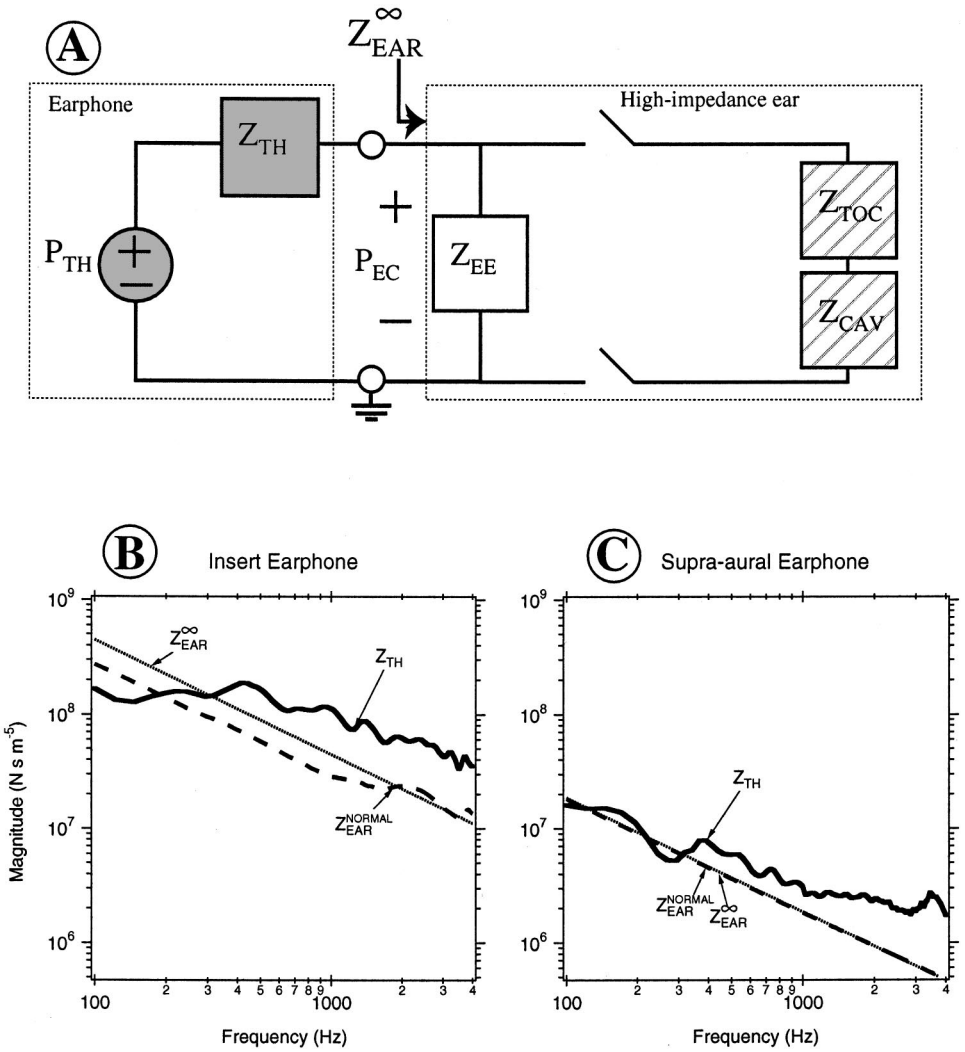

FIG. 9. (A) Model for an ear with a pathology that results in an infinite impedance magnitude at the tympanic membrane. Here, the impedances that represent the middle-ear are disconnected by an open switch. The impedance Z_{EE} that represents the ear-canal air–space is identical to the normal middle ear of Fig. 5(A). Z_{EAR} is the driving-point impedance of the ear and suprascripts refer to the ''normal-'' and the ''infinite-'' impedance conditions. (B) and (C) Impedance values for the model above with the insert earphone (B) and the supra-aural earphone (C).

ior is similar to the condition with the tube. At the lowest frequencies, the driving-point impedance magnitude $|Z_{\mathrm{EAR}}^{\mathrm{PERF}}|$ is essentially the parallel combination of the compliance-dominated impedances Z_{EE} and Z_{CAV}. As frequency increases, a minimum and maximum occur in $|Z_{\mathrm{EAR}}^{\mathrm{PERF}}|$, as with the tymanostomy tube. A series resonance between the perforation's mass and the effective middle-ear cavity compliance results in an impedance minimum, and a parallel resonance between the external-ear volume and the effective middle-ear cavity compliance and the perforation's mass results in an impedance maximum. Thus, as in the case with the tube, the frequency of the impedance minimum is independent of the earphone, and the frequency of the impedance maximum depends on the earphone. The condition (Sec. C) of the Introduction) required for constant ear-canal pressures—that variations in Z_{EAR} must be small relative to $Z_{\mathrm{EAR}}^{\mathrm{NORMAL}}$—is not met at some lower frequencies.

5. ''High-impedance'' ear

Pathologies that can increase the impedance of the ear include otosclerosis and a fluid-filled middle-ear cavity. An ''infinite-impedance'' middle ear represents an upper limit for the effect of pathologies that increase the ear's impedance: with the impedance magnitude at the tympanic membrane infinite,[6] the earphone's load impedance is that of the ear-canal air space Z_{EE} [Fig. 9(A)].

In Fig. 9(B) and (C), the effect of the ''infinite-impedance'' middle ear is shown for each earphone. The impedance magnitude that the earphone must drive, $|Z_{\mathrm{EAR}}^{\infty}|$, increases relative to $|Z_{\mathrm{EAR}}^{\mathrm{NORMAL}}|$ with both earphones, but not by a large factor. For the insert earphone, the impedance increases by less than a factor of 2 at all but the lowest frequencies, and for the supra-aural earphone, the impedance increases by an indistinguishable amount. The reason for these small impedance changes is that the external-ear volume limits the driving-point impedance. With this external-ear ''buffer,'' the impedance that the earphone must drive can never exceed the impedance of the external-ear volume. For example, with the insert earphone, at 1000 Hz, the second term of Eq. (2) is $(\Delta Z_{\mathrm{EAR}}/Z_{\mathrm{EAR}}^{\mathrm{NORMAL}})/(1+Z_{\mathrm{EAR}}/Z_{TH}) \approx 0.45$, so that $|P_{\mathrm{EC}}/P_{\mathrm{EC}}^{\mathrm{NORMAL}}| \approx 1.45$, and the sound pressure in the ear is only about 3 dB greater than the assumed calibration value. Thus, for ears with pathologies that increase the impedance magnitude, variations in $|Z_{\mathrm{EAR}}^{\infty}|$ relative to $|Z_{\mathrm{EAR}}^{\mathrm{NORMAL}}|$ are small and the condition that variations in Z_{EAR} must be small relative to $Z_{\mathrm{EAR}}^{\mathrm{NORMAL}}$ is met.

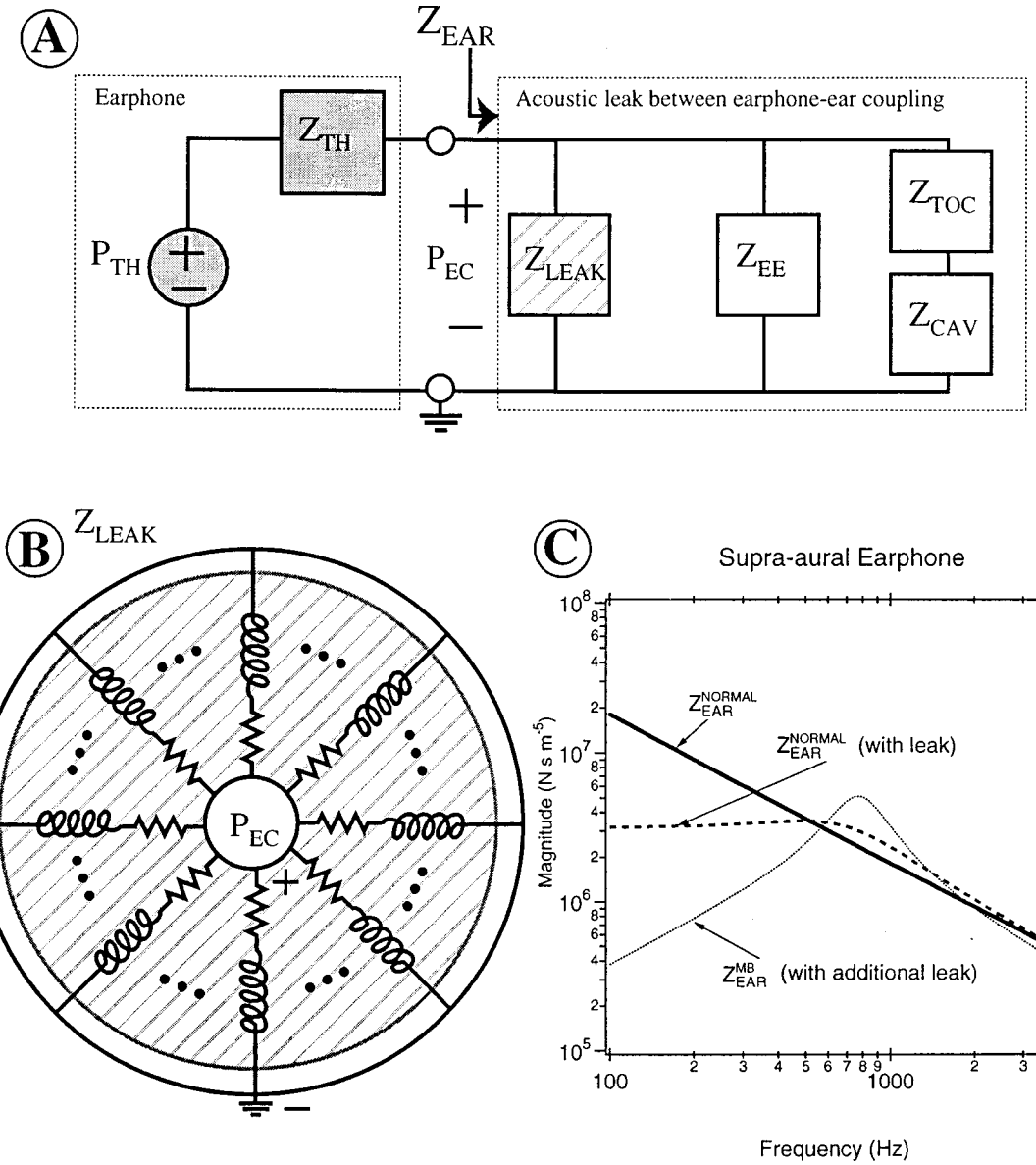

FIG. 10. (A) Model for a normal ear with a leak between the earphone and the ear. The impedances Z_{EE}, Z_{TOC}, and Z_{CAV} are identical to the normal middle ear of Fig. 5(A). The impedance labeled Z_{LEAK} (striped) represents the leak. (B) Model for the acoustic leak. The striped annular region represents the cushion of a supra-aural earphone, across which there are several small pathways that connect the air in the center of the cushion to the surrounding air. Here, eight independent air pathways are represented, each by a frequency-dependent acoustic mass in series with a frequency-dependent acoustic resistance. The three dots between each air pathway indicate the possibility of more elements in the array. The calculations shown here use 150 total pathways so that $Z_{\mathrm{LEAK}}=(1/150)[R_{\mathrm{LEAK}}(f)+j\omega M_{\mathrm{LEAK}}(f)]$. (C) Model predictions for the driving-point impedance magnitude for the normal ear with and without the leak shown here $|Z_{\mathrm{EAR}}^{\mathrm{NORMAL}}|$ [array of 150 ''tubelike'' leaks as in (B)] and the driving-point impedance magnitude for a mastoid-bowl ear $|Z_{\mathrm{EAR}}^{MB}|$ with an additional larger leak described in the text.

D. Acoustic leaks between the earphone and the ear

As demonstrated later [Fig. 11(B) and Fig. 13], our measurements with the supra-aural earphone (Voss *et al.*, in press) are consistent with acoustic leaks occurring at the earphone-ear connection. Here, we propose circuit models for the supra-aural earphone configuration with an acoustic leak in the earphone-ear connection with a normal ear and with an ear with a mastoid bowl. We do not know the spatial configuration of the leaks, which probably differ among ears; our models for the normal and the mastoid-bowl ears represent possible leak configurations.

To motivate the configuration of our model [Fig. 10(A)], consider the connection between a supra-aural earphone and a normal ear. For no leaks to occur, around its entire periphery the earphone cushion must abut the pinna. Here, we propose a model in which gaps occur between the pinna and the cushion in the normal ear. We represent these connections to the space around the earphone as an array of small tubes ($N=150$), indicated schematically in Fig. 10(B), each with a length $l_{\mathrm{leak}}=2.5\,\mathrm{cm}$, which corresponds to the distance from the central hole of the earphone cushion to its outer edge, and a radius $r_{\mathrm{leak}}=0.0125\,\mathrm{cm}$ (for a total leak area of $150\pi r_{\mathrm{leak}}^2=0.08\,\mathrm{cm}^2$). The impedance for each tube in the array is calculated from the lossy equations of Egolf (1977) with a terminating impedance of zero.[7] Each tube in the array is indicated schematically in Fig. 10(B) by a frequency-

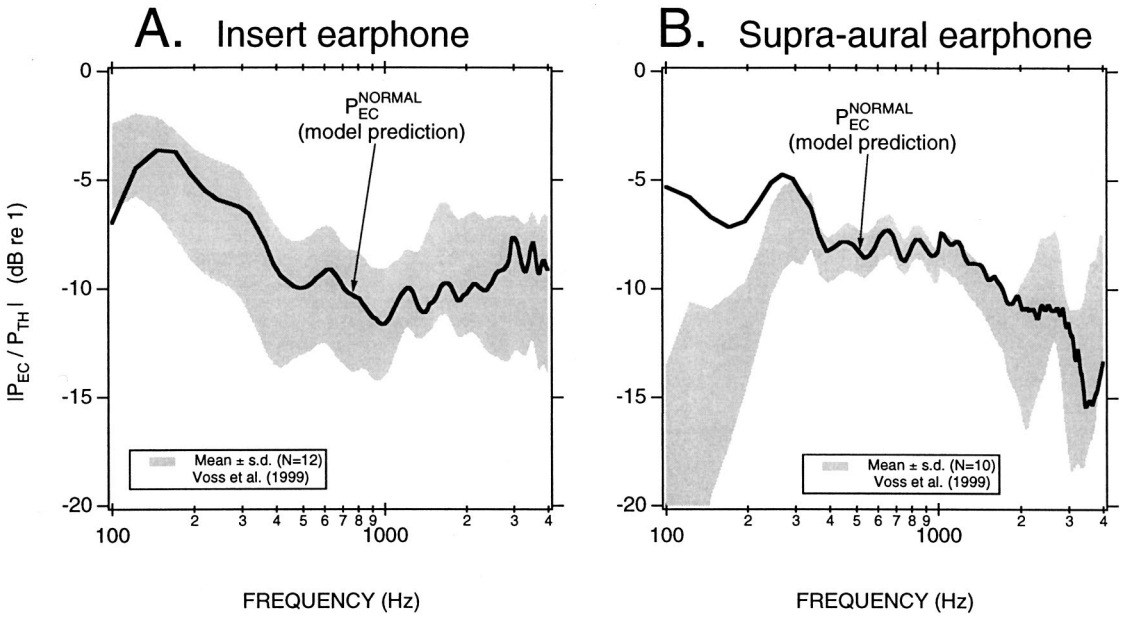

FIG. 11. Normal ears: Ear-canal pressure relative to the Thévenin equivalent P_{TH} for the insert earphone (A) and the supra-aural earphone (B). Solid lines are model predictions for the normal ear using the model of Fig. 5(A). Gray-shaded regions are the means plus and minus one standard deviation from measurements on populations of subjects with normal ears. The vertical scale is $20\log_{10}(|P_{EC}/P_{TH}|)$.

dependent mass in series with a frequency-dependent resistance. These leak-model parameters were chosen because they produce an ear-canal pressure that matches average measurements made on normal ears with the supra-aural earphone. Other leak configurations that match the measurements can also be found, as there are several free parameters in this model (i.e., r_{leak}, l_{leak}, N). With the leak configuration proposed here, Fig. 10(C) shows that the ear's driving-point impedance magnitude (with a leak) is reduced for frequencies below 500 Hz, slightly increased for frequencies between 500 and 1000 Hz due to a parallel resonance between the mass of the leak and the compliance of the normal ear, and roughly normal for frequencies above 1000 Hz where the leak's impedance magnitude becomes much greater than the ear's normal impedance magnitude and as a result the leak is effectively plugged.

Our measurements of ear-canal pressures generated by the supra-aural earphone show the largest low-frequency reductions in ear-canal pressure in ears with mastoid bowls, suggesting that larger leaks occur with mastoid-bowl ears than with other types of ears. (Reasons for these larger leaks are discussed below in Sec. III D.) We model the additional leak as a single pathway between the air space under the earphone cushion and the atmosphere. This pathway, which is larger than any of the single pathways for a leak with a normal ear, is represented by an acoustic mass $M_{\text{leak}}^{MB}=\rho_{\text{leak}}^{MB}/A_{\text{leak}}^{MB}$ whose impedance is calculated as $Z_{\text{leak}}^{MB}=j\omega M_{\text{leak}}^{MB}$. Figure 10(C) shows the predicted driving-point impedance for an ear with a 3-cm^3 mastoid bowl, an array of small leaks identical to those shown for the normal ear, and an additional leak with $l_{\text{leak}}^{MB}=1$ cm and $A_{\text{leak}}^{MB}=0.2$ cm^2 that is placed in parallel with the leak for the normal ear. Figure 10(C) shows that with the given configuration, the mastoid-bowl ear's driving-point impedance magnitude is reduced for frequencies below 500 Hz (by nearly a factor of 100 at 100 Hz), increased relative to normal for frequencies between 500 and 1500 Hz, and nearly unchanged for frequencies above 1500 Hz.

III. MODEL PREDICTIONS

A. Plan

In this section, we use the models to predict the ear-canal pressure generated in each of the two earphone configurations in normal and pathologic ears. We are particularly interested in showing how the ear-canal pressures change from normal when the ear's impedance changes due to pathology or when an acoustic leak exists between the ear and the supra-aural earphone; thus, we plot ear-canal pressures relative to those in normal ears [i.e., Eq. (2)]. We include measurements (Voss *et al.*, in press) with the model predictions where possible.

B. The normal ear

In Fig. 11 measurements are compared to the model predictions (with no representation of a leak at the earphone-ear connection) for normal ears. For an earphone that acts as an ideal pressure source, the ratio $|P_{EC}/P_{TH}|$ would correspond to 0 dB (i.e., $P_{EC}=P_{TH}$). In Fig. 11, the measurements show that with either earphone $|P_{EC}/P_{TH}|<-5$ dB for most frequencies, and thus neither earphone approximates an ideal pressure source. The model predictions for the insert earphone approximate the mean of the measurements and are within one standard deviation of the mean at most frequencies; thus, the model predictions are consistent with the measurements. In contrast, the model predictions for the ear-canal pressures generated by the supra-aural earphone are consistent with the measurements above 250 Hz, but below 250 Hz the measurements and model differ by about 10 dB.

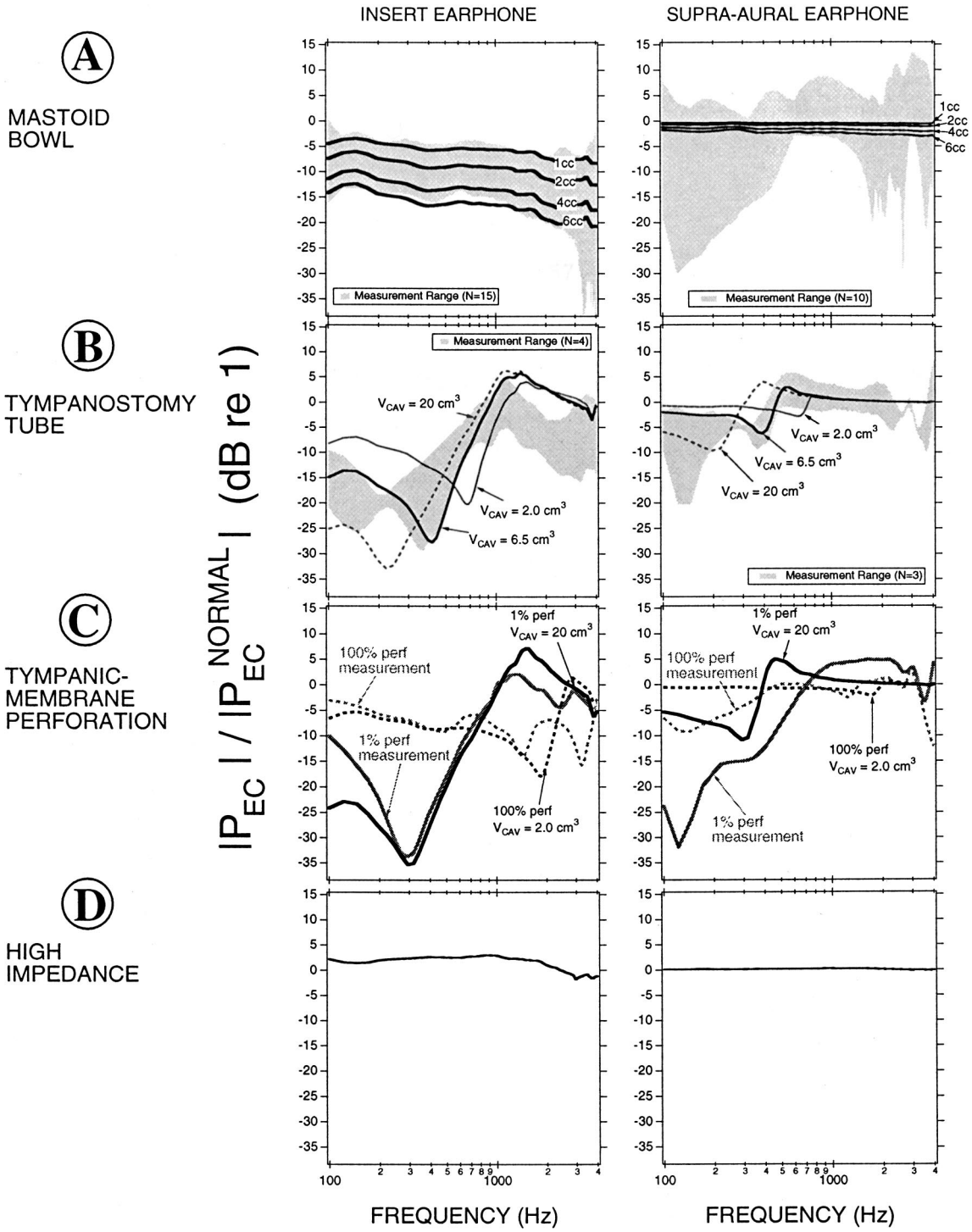

FIG. 12. Model predictions for the ear-canal pressures generated in ears with middle-ear pathologies with the insert earphone (LEFT) and the supra-aural earphone (RIGHT). Pressures are in dB relative to the pressure generated in a normal ear (Fig. 11). All model predictions are in black lines. Gray shaded regions (lines) indicate the range (value) of measurements made on subjects (Voss *et al.*, 1999). (A) Mastoid-bowl ears. (B) Tympanostomy-tube ears. The measurement ranges summarize measurements on ears with Baxter™ tympanostomy tubes. Model predictions are shown for three choices of middle-ear cavity volume V_{CAV}. (C) Perforations of the tympanic membrane. The perforation diameter was estimated visually, using an otoscope, for the human subjects, and the model's middle-ear cavity volume V_{CAV} was selected to fit the measurements. The 100% perforation refers to a case with no tympanic membrane. (D) ''High-impedance'' ear. No measurements were made for this condition. In the model (Fig. 9) $|Z_{TOC}+Z_{CAV}|$ was made infinite.

An explanation of this difference in terms of a leak between the earphone's cushion and the ear will be discussed further in Sec. III D below. As measurements made by Shaw (1966, Fig. 2) with the TDH supra-aural earphone show a similar low-frequency difference between pressures generated in a coupler and pressures generated in normal ears, this result seems to be representative of other measurements.

C. Pathologic ears

1. Mastoid bowl

a. Model predictions. The model predicts [Fig. 12(A)] that a mastoid bowl reduces the ear-canal pressure generated by both the insert and the supra-aural configurations and that the pressure reduction increases as mastoid-bowl volume in-

creases; the reduction is much greater with the insert earphone than with the supra-aural earphone. With the insert earphone and a mastoid bowl of 6 cm^3, the reduction is between 15 and 20 dB, whereas with the supra-aural earphone it is only 2–3 dB. This difference is a consequence of the impedances shown in Fig. 7: The volume of the mastoid bowl has dramatic effects on the driving-point impedance Z_{EAR} with an insert earphone because the insert earphone faces an external-ear volume of only 0.5 cm^3; addition of the 6-cm^3 bowl increases the total volume by a factor of 12. Conversely, with the supra-aural earphone the external-ear volume of 12.0 cm^3 is increased by only a factor of 1.5 by the 6-cm^3 bowl, which changes the impedance magnitude $|Z_{EAR}|$ by a factor of about 0.7 (or -1 dB) at all frequencies.

b. Comparison to measurements. Measurements of ear-canal pressures made on human subjects are generally consistent with the model predictions [Fig. 12(A)]. For the insert earphone, the measurement range is very close to the model's range for volumes of 1 cm^3 to 6 cm^3. With the supra-aural earphone, the range of the measurements is much larger than the model predictions, with both a systematic reduction in pressure below about 500 Hz and increases in pressure between 500 and 1000 Hz; these features could result from acoustic leaks between the earphone cushion and the ear; this possibility is discussed in Sec. III D.

Differences between the measurements and the supra-aural earphone model predictions also occur at frequencies above 1000 Hz. Here, the ear-canal pressure measurements (individual measurements are shown in Fig. 14) show sharp pressure extrema that differ by at least 15 dB from the range of pressures measured in the normal ears; these extrema are not predicted by our simple lumped model, whose validity at these frequencies was questioned earlier (Sec. II A). These extrema are further discussed in Sec. III E below in terms of a more complex model.

2. Tympanostomy tube

a. Model predictions. The model predicts that a tympanostomy tube introduces a low-frequency minimum in ear-canal pressure (relative to a normal ear) which depends on the volume of the middle-ear cavity as well as the tube's dimensions [Fig. 12(B)]. For frequencies above 1000 Hz, the changes from normal are less than 5 dB in both earphone configurations. Model predictions are plotted for an average size middle-ear cavity of 6.5 cm^3 and two extreme volumes that correspond to the range of anatomical measurements in a population of normal temporal bones: 2.0 cm^3 and 20 cm^3 (Molvaer *et al.,* 1978). The changes in ear-canal pressure are again larger for the insert earphone than for the supra-aural earphone, but the general behavior is similar for the two earphones. As the middle-ear cavity volume increases, both the frequency and the level of the pressure minimum decrease. For the same middle-ear cavity volume, the two earphone configurations have pressure minima at the same frequency.

b. Comparison to measurements. Measurements of the ear-canal pressures made on human subjects with Baxter™ tympanostomy tubes are consistent with the model predictions shown here. The gray shaded regions of Fig. 12(B) indicate the range of measurements on a small population of subjects (insert earphone $N=4$; supra-aural earphone $N=3$). Because the model predictions are highly dependent on the middle-ear cavity volumes, which are unknown in the patient population, it is impossible to compare an individual measurement to the model. With anatomically reasonable volume variations, the supra-aural earphone model predicts the measured range, and the insert-earphone model predicts the measured range for frequencies below about 1000 Hz and pressures that are 5–10 dB greater than the measurements for frequencies above 1000 Hz. One explanation for this 5–10 dB difference between the model predictions and the measurements involves the choice of the model parameters. In the model, the component Z_{TOC} is determined from temporal-bone measurements on normal ears (Fig. 5). However, the measurements in Fig. 12(B) are from ears with histories of middle-ear disease, which can reduce the stiffness of the tympanic membrane (Unge *et al.,* 1995). In fact, reducing the model $|Z_{TOC}|$ does result in a reduced ear-canal pressure that more closely approximates the measurements in the 1000–4000 Hz range. Variations of Z_{TOC} from normal are also likely in ears with tympanic-membrane perforations, but the issue is less important in ear's with mastoid bowls because with a mastoid bowl, the additional ear-canal volume dominates the ear's input impedance to frequencies greater than 4000 Hz.

Measurements with both an insert earphone and a supra-aural earphone were made on three subjects with Baxter™ tympanostomy tubes. As the model predicts, low-frequency pressure minima occurred at the same frequencies with both earphones (Fig. 4 of Voss *et al.*, in press).

3. Tympanic-membrane perforations

a. Model predictions. According to the model, the changes in the ear-canal pressure generated with a perforated tympanic membrane depend on both the middle-ear cavity volume and the diameter of the perforation. Model predictions are plotted [Fig. 12(C)] for perforations of two extreme sizes for which we also have measurements: 1% and 100% of the tympanic-membrane area. As we do not have measurements of the middle-ear cavity volumes in individual subjects, volumes were chosen to make the model prediction and the measurement similar.[8] In general, the smaller perforation behaves similarly to the tympanostomy tube: A low-frequency pressure minimum occurs at the same f_{min} for both earphones, and the pressure minimum is smaller with the insert earphone than with the supra-aural earphone. The larger perforations behave more like mastoid bowls with a relatively constant loss as a function of frequency.

b. Comparison to measurements. Figure 12(C) compares model predictions for two perforations with measurements of ear-canal pressure in ear canals with the same size perforations (1% and 100% perforations). Here, we plot individual measurements instead of measurement ranges, because the perforation diameter, which is a parameter in our data, has a large effect on the ear-canal pressure. Just as with the tympanostomy-tube case, model predictions using

middle-ear cavity volumes consistent with the normal range of anatomical measurements are similar to the measured values. An exception occurs with the supra-aural earphone at the lowest frequencies where the measured pressure with a 1% perforation is substantially below the (no leak) model.

4. High-impedance ear

Figure 12(D) shows model predictions for a ''high-impedance'' ear. The predicted ear-canal pressure generated by either earphone is no more than 3 dB greater than in the normal ear. As described above (Sec. II C 5), the maximum driving-point impedance magnitude $|Z_{\mathrm{EAR}}|$ is limited by the volume of the external ear. Thus, with either earphone, the terminating impedance magnitude $|Z_{\mathrm{EAR}}|$ can only increase a small amount when $|Z_{\mathrm{TOC}}+Z_{\mathrm{CAV}}|$ goes to infinity and the ear-canal pressure remains nearly unchanged. [For the highest frequencies shown, 2000–4000 Hz, there is a slight reduction in pressure with the insert-earphone configuration attached to the ''high-impedance'' ear because at these frequencies the magnitude of the impedance of the external-ear space is less than the magnitude of the normal ear impedance (Fig. 9).]

Our conclusion that a high-impedance ear has only small effects on ear-canal pressures depends on the volume of the external ear, i.e., the conclusion assumes that the external-ear volume is that of a normal adult-sized ear with $V_{EE}^{I}=0.5\,\mathrm{cm}^3$ for the insert earphone or $V_{EE}^{SA}=12\,\mathrm{cm}^3$ for the supra-aural earphone. Here we consider the effects of extreme changes in these volumes on ear-canal pressures. For example, consider the case of a smaller volume, as may be appropriate for a young child with a shorter and narrower ear canal than an adult (Keefe *et al.*, 1993). As V_{EE} approaches zero, the ear-canal pressure will be determined by the impedance of the middle ear. In the limiting case, with a high-impedance middle ear, the earphone's terminating impedance will be high and the ear-canal pressure will approach the Thévenin pressure P_{TH}. As shown in Fig. 11, the pressures generated in normal ears are only 5–10 dB below P_{TH}; thus, a small V_{EE} coupled with a high-impedance middle ear can never increase the ear-canal pressure by more than about 10 dB.

D. Acoustic leaks between the earphone and ear

At frequencies below 250 Hz, the ear-canal pressures generated by a supra-aural earphone in normal ears were smaller than those predicted by our (leak free) model [Fig. 11(B)]. Figure 13 compares these results of Fig. 11(B) to the model prediction with the array of small ''tubelike'' leaks (Sec. II D) between the pinna and the supra-aural earphone cushion. The model predictions with this array of small leaks is consistent with the measurements and with the hypothesis that the supra-aural earphone is difficult (if not impossible) to seal acoustically around the pinna and as a result there are low-frequency pressure reductions in ear-canal pressure. We conclude that there are always small acoustic leaks between a supra-aural earphone and a pinna that result in reduced ear-canal sound pressures at frequencies below about 250 Hz. In support of this conclusion, we note that our measurements on ten subjects all showed smaller ear-canal pressures

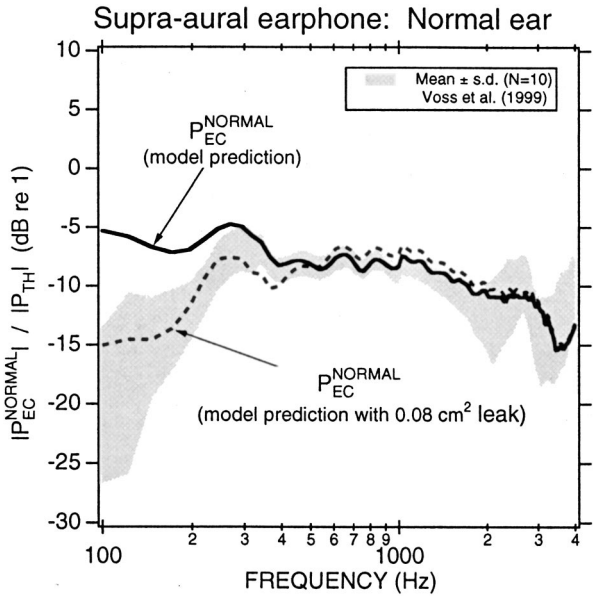

FIG. 13. Model predictions for ear-canal pressures (relative to the earphone's Thévenin pressure P_{TH}) generated in a normal ear when there is a leak between the cushion of the supra-aural earphone and the pinna. Model for the leak has an array ($N=150$) of ''tubelike'' leaks, each with $r_{\mathrm{leak}}=0.0125$ cm and $l_{\mathrm{leak}}=2.5$ cm. Also shown is the model prediction for the normal ear with no leak. The gray shaded region is the mean plus and minus one standard deviation from the measurements on 10 normal ears (Voss *et al.*, in press).

than predicted by our model, and measurements of ear-canal pressure in ten ears made by Shaw (1966, Fig. 2) were all reduced relative to the pressure measured in a coupler.

Our measurements of ear-canal pressures in ears with mastoid bowls show large reductions at low frequencies that are also not accounted for by our model of a mastoid-bowl cavity [Fig. 12(A)]. These pressure reductions are consistent with larger acoustic leaks in the earphone-to-ear connection than the leaks proposed for a normal ear. Effects of the surgery might lead to larger leaks with mastoid-bowl ears. The surgery includes an incision in the skin behind the pinna. As the incision heals, the scar can pull the posterior portion of the pinna flange closer to the skull. This ''bent'' configuration may introduce a larger leak between the supra-aural earphone cushion and pinna flange (Merchant, 1999).

Figure 14 compares the ear-canal pressures generated by the supra-aural earphone in three ears with mastoid bowls to our model prediction for a leak in the earphone-to-ear connection of a mastoid-bowl ear. The model includes two types of leaks: the array of small ''tubelike'' leaks that accounts for the normal ear's earphone-to-ear connection [Fig. 10(B)] and one larger leak that might occur in a region where the earphone cushion does not parallel the pinna. The model has features that are generally consistent with most of the measurements: the pressure reductions are greatest at the lower frequencies and increases with frequency until a maximum is reached around 500 Hz. It is possible to predict ear-canal pressures with features consistent with each measurement by associating an appropriate ''leak area'' and ''leak length'' with the measurement; measurements with the larger low-frequency pressure reductions have larger leak areas and measurements with the smaller low-frequency pressure re-

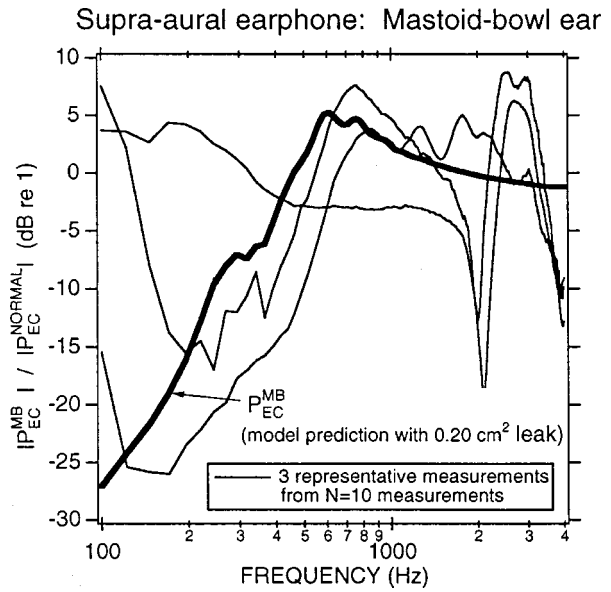

FIG. 14. Model predictions for ear-canal pressures generated in ears when there is a leak between the cushion of the supra-aural earphone and the pinna of a mastoid-bowl ear (bowl volume 3 cm^3) with both the same array of ''tubelike'' leaks shown in Fig. 13 and one additional larger leak (one tube-shaped leak with area 0.12 cm^2 and length 1 cm^2). Also shown are three measurements selected from a total of ten measurements made on mastoid-bowl ears (thin black lines); these three measurements are representative of the total range and general shape of all measurements (Voss *et al.*, in press).

ductions have smaller leak areas associated with them. We conclude that most of our measurements made on mastoid-bowl ears are consistent with larger-than-normal leaks in the earphone-to-ear connection of the supra-aural earphone.

E. Sharp pressure extrema with a supra-aural earphone and a mastoid-bowl ear

Our measurements of ear-canal pressures generated by the supra-aural earphone coupled to ears with mastoid bowls exhibit sharp pressure extrema that typically include a pressure minimum near 2000 Hz of about -20 dB (relative to normal) and a pressure maximum near 2500 Hz of about 10 dB (relative to normal) [Fig. 14 and Fig. 3 from Voss *et al.* (in press)]. Such sharp pressure extrema are not seen in either (1) the measurements on normal ears [Fig. 11(B) and Fig. 2 from Voss *et al.* (in press)] or (2) the model predictions shown with our ''simple'' lumped-element model of Fig. 7(A). Here, we propose an amendment to the model that predicts these pressure extrema at the higher frequencies without affecting the low-frequency behavior with the supra-aural earphone and mastoid-bowl cavity configuration.

As discussed in Sec. II C 2, the ''simple'' lumped-element model with the supra-aural earphone and mastoid-bowl cavity configuration becomes inaccurate at frequencies above 1000 Hz, where the dimensions of the external-ear air volume approach the wavelength of sound. Here, we increase the model's frequency range by adding elements to allow a pressure change along the ear canal between the air space under the earphone and the concha to the mastoid-cavity volume [Fig. 15(A)]. Instead of representing the external-ear air space as a lumped compliance with volume $V_{EE}=12$ cm^3 [i.e., as in Fig. 7(A)], we separate this total air volume into three regions: 1. The air volume within the concha and under the supra-aural earphone cushion ($V'_{EE}=11$ cm^3) is represented by C'_{EE}; 2. The ear canal itself is represented as a ''Π'' network where two compliances—each equal to $0.5C_{EC}$ and representing one-half of the ear-canal volume—are connected by an acoustic mass M_{EC} that is determined by the ear-canal dimensions, $M_{EC}=\rho l_{EC}/(\pi r_{EC}^2)$, where l_{EC} is the ear-canal length and r_{EC} is the ear-canal radius; and 3. The air volume of the mastoid-bowl cavity is represented by the compliance C_{BOWL}.

Here, we choose model-element values for the distributed model [Fig. 15(A)] of the external ear with a mastoid bowl. Values for C'_{EE} and C_{BOWL} are obtained from equivalent volumes defined in the preceding paragraph. The ear-canal dimensions determine the values for the M_{EC} and the $0.5C_{EC}$ of the ''Π'' network. After mastoid surgery, the ear canal is often wider-than-normal, and the canal is shorter-than-normal because the ''tubelike'' part of the canal is terminated by the mastoid-bowl cavity. To define M_{EC} for a mastoid-bowl ear, we use an ear-canal length $l_{EC}^{MB}=1.0$ cm and an ear-canal radius $r_{EC}^{MB}=0.56$ cm. These dimensions also define $0.5C_{EC}=0.5V_{EC}/(\rho c^2)$, where $V_{EC}=1.0$ cm^3 is the ear-canal volume, which is equal to the ear-canal volume computed for a normal ear with average dimensions (i.e., an ear-canal length $l_{EC}^{\mathrm{NORMAL}}=2.5$ cm and an ear-canal radius $r_{EC}^{\mathrm{NORMAL}}=0.36$ cm).

For frequencies below 1000 Hz, the ''distributed model'' [Fig. 15(A)] and the ''simple'' model [Fig. 7(A)] make the same predictions for the ear-canal pressure with a mastoid-cavity bowl [Fig. 15(B)]. Only as frequency increases above 1000 Hz do spatial variations become significant and the ''distributed'' representation of the ear canal has large effects on the model predictions compared to the ''simple'' model [Fig. 15(B)]. In particular, the distributed ear-canal model leads to sharp pressure extrema, with a pressure minimum that results from a series resonance between the mass of the ear canal and the compliance of the mastoid-bowl cavity and a pressure maximum that results from a parallel resonance between the mass of the ear canal and the compliances of the external ear and the mastoid-bowl cavity. As indicated in Fig. 15(B), the volume of the mastoid bowl influences the frequencies of the model's pressure extrema, with the larger mastoid-bowl volume producing extrema at lower frequencies. Since these pressure extrema are similar in magnitude and frequency to those measured on subjects with mastoid bowls [Fig. 14 and Fig. 3 of Voss *et al.* (in press)], we conclude that the pressure extrema result from resonances between the ear-canal and the air spaces of the external ear and the mastoid bowl.

Next, we test whether our ''simple'' model for the normal ear is adequate for the frequency range 100–4000 Hz that we have considered. A distributed model for the external ear of a normal ear is similar to the model for the mastoid-bowl ear [Fig. 15(A)] except the compliance that represents the mastoid bowl, C_{BOWL}, is removed, and the dimensions of the ear canal that define M_{EC} and $0.5C_{EC}$ correspond to a normal ear canal (i.e., an ear-canal length $l_{EC}^{\mathrm{NORMAL}}=2.5$ cm and an ear-canal radius $r_{EC}^{\mathrm{NORMAL}}=0.36$ cm). With a normal

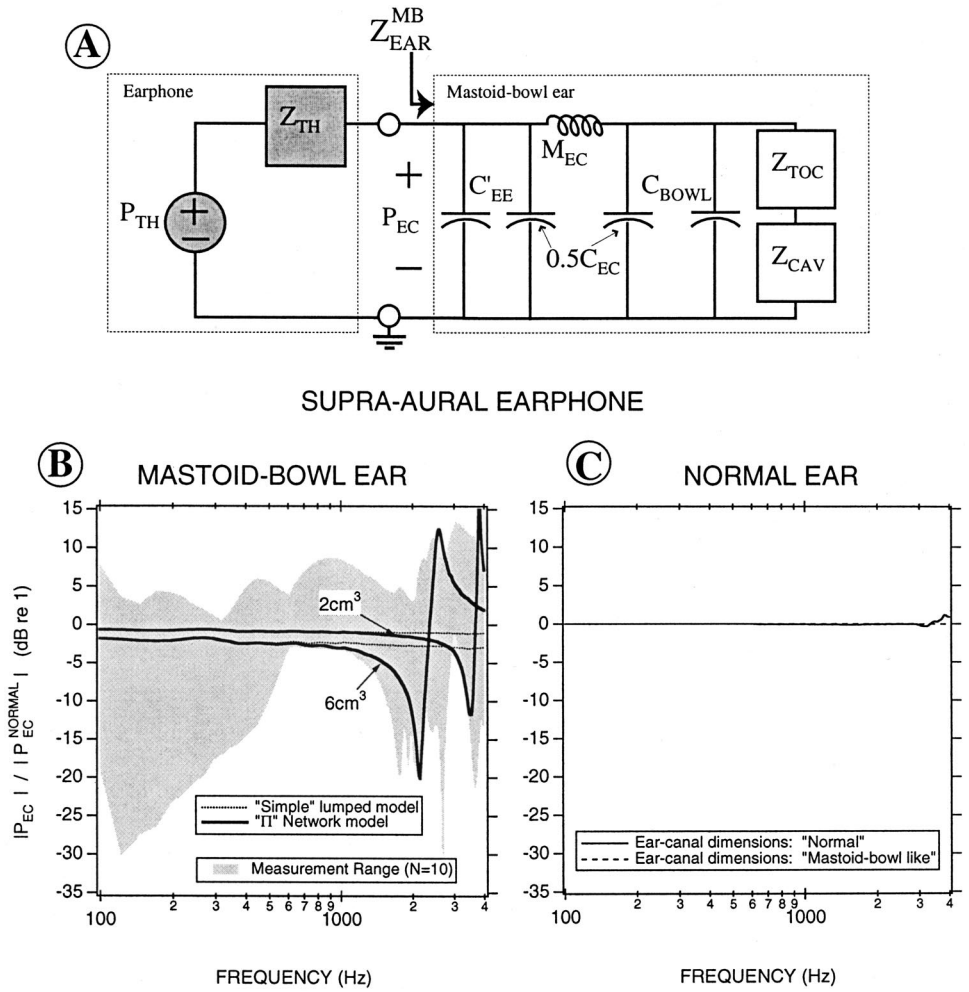

FIG. 15. (A) Modified representation of the external-ear air volume in the model of the supra-aural earphone coupled to a mastoid-bowl ear. The ear canal is modeled as a ''Π'' network with two compliances ($0.5C_{EC}$) connected by mass M_{EC}. The external-ear air volume lateral to the ear canal and the mastoid-bowl cavity remain represented by compliances: C'_{EE} and C_{BOWL}, respectively. (B) Model predictions for the mastoid-bowl ear with the ear-canal represented by both the simple model of Fig. 7(A) (dotted lines) and the ''Π'' network defined above (solid lines) with ear-canal dimensions for a mastoid-bowl ear (i.e., $l_{EC}=1.0$ cm; $r_{EC}=0.56$ cm). Model predictions are shown for two bowl volumes (2 cm^3 and 6 cm^3). The model predictions for each bowl volume (indicated on plot) overlap at the lowest frequencies. (C) Model predictions for the normal ear with the ear-canal represented by the ''Π'' network defined above relative to the model predictions with the simple model of Fig. 5(A). The solid line are calculations made with ear-canal dimensions of a normal ear (i.e., $l_{EC}=2.5$ cm; $r_{EC}=0.36$ cm), and the dashed lines are calculations made with ear-canal dimensions of a mastoid-bowl ear (i.e., $l_{EC}=1.0$ cm; $r_{EC}=0.56$ cm), where both sets of ear-canal dimensions result in an ear-canal volume of 1.0 cm^3.

ear, the two model topologies (i.e., the ''simple'' lumped model and the distributed model) predict nearly identical ear-canal pressures [Fig. 15(C)]. Additionally, as shown in Fig. 15(C), the dimensions of the ear canal have little effect on the model prediction as long as the total volume is constant (i.e., l_{EC}^{NORMAL} and r_{EC}^{NORMAL} lead to model predictions that are nearly identical to model predictions made with l_{EC}^{MB} and r_{EC}^{MB}). Thus, for a supra-aural earphone coupled to a normal ear, the ''simple'' lumped external-ear compliance is adequate and the distributed representation of the ear canal is unnecessary for frequencies up to 4000 Hz.

IV. DISCUSSION

A. Summary of results

Our lumped-element model explains how the sound pressure generated in abnormal ears differs from normal. These differences can lead to significant errors in hearing tests, when it is assumed that the earphone produces the same sound-pressure level in all tested ears.

Middle-ear pathology can both increase and decrease the ear's impedance relative to normal. Both an insert-earphone model and a supra-aural-earphone model predict that ear-canal pressures will be altered when the impedance of the middle ear is reduced. In general, changes from normal are larger with the insert earphone because the insert-earphone's small external-ear volume (relative to the supra-aural earphone) results in a higher load impedance which can be greatly reduced as a result of pathology (mastoid bowl, tympanostomy tube, tympanic-membrane perforation). On the other hand, when the ear's impedance magnitude increases relative to normal, the ear-canal pressure generally increases by less than 3 dB relative to normal, because the impedance of the air–space volume between the tympanic membrane and the earphone generally places an upper limit on the load impedance on the earphone.

The earphone's output can also be affected by acoustic leaks between the ear and the earphone. Here, our supra-aural earphone model predicts that such leaks lead to reduced ear-canal sound pressures at low frequencies and slightly increased ear-canal pressures near the resonant frequency between the mass of the leak and the compliance of the ear's load.

B. Pressure in the ear canal versus pressure at the tympanic membrane

We have focused on variations in the ear-canal pressure P_{EC} generated at the output of the earphone. Inter-ear variations in the pressure generated by the earphone—at the earphone's location—are important to quantify because they are currently assumed negligible when testing hearing.

Another fundamental issue that remains to be addressed deals with determining whether generating a constant sound pressure in the external ear leads to an accurate test of hearing acuity for all ears. For example, at higher frequencies, standing waves can be generated in the ear canal, and the pressure generated at the earphone may not be representative of the pressure at the tympanic membrane. Neely and Gorga (1998) have recently suggested that sound intensity level might provide a more useful measure than sound-pressure level in these circumstances.

Another possibility for improved hearing testing would be to test hearing with free-field sound. In this way, effects of ear-canal standing waves and external-ear filtering would be included in the hearing test in a manner similar to real-world hearing situations.

C. Insert versus supra-aural earphones

Differences between insert earphones and supra-aural earphones have been discussed extensively in the literature. In general, supra-aural earphones are purported to have a larger high-frequency dynamic range than many insert earphones (Zwislocki *et al.*, 1988), while insert earphones provide several advantages over supra-aural earphones, including the reduction of leaks in the earphone-to-ear connection and increased interaural attenuation (Killion and Villchur, 1989). Our measurements and models show advantages and disadvantages for both the insert and the supra-aural earphones. The ear's impedance has a larger effect on the sound pressure generated by the insert earphone than by the supra-aural earphone. Variations in low-frequency pressures that result from leaks are a bigger problem with supra-aural earphones than with insert earphones. We also expect variations in pressure along the ear canal to be larger with supra-aural earphones than with insert earphones as a result of the larger distance between the earphone and the tympanic membrane with the supra-aural earphone.

D. Conclusions

Our model represents mechanisms that can cause systematic ear-canal pressure variations of up to 35 dB in abnormal ears relative to normal; in many cases, pressure variations are as much as 15 dB at several frequencies. To reduce the problem of unknown variations in ear-canal sound-pressure levels, a microphone to monitor ear-canal pressures could be built into commercial audiometers, as suggested many years ago (Harris, 1978). The addition of such a microphone to an insert earphone would result in a system that maintains all of the advantages of an insert earphone and also controls ear-canal pressures close to the tympanic membrane; such a microphone is also a necessary feature of an audiologic system designed to measure the sound intensity level in the ear canal. The models presented here can be used to help define the range of ear-canal pressures such a system would need to correct.

ACKNOWLEDGMENTS

This work was supported by training and research grants from the NIDCD. We thank two anonymous reviewers for helpful comments.

[1]According to Sadé (1982), tympanic-membrane perforations affect 0.5%–30% of any community.

[2]It is estimated that 1.3% of American children (aged 8 months to 16 years) have tympanostomy tubes at a given time (Bright *et al.*, 1993).

[3]The ear canal has a length of about 28 mm and a diameter of about 7 mm (Wever and Lawrence, 1954, pp. 416). The insert earphone assembly extends about 15 mm into the ear canal: the 12 mm length of the foam plug plus 3 mm for the probe-tube extension. Thus, the ear-canal volume between the probe tube and the tympanic membrane accounts for the external-ear air volume of $V_{EE}^{I}=0.5\ \mathrm{cm}^3$. The supra-aural earphone couples to the ear via a cushion that rests along the edge of the pinna. Here, we use a total external-ear air volume of $V_{EE}^{SA}=12\ \mathrm{cm}^3$, where 1.0 cm^3 accounts for the ear-canal volume (Shaw, 1974), 4.0 cm^3 accounts for the concha volume (Shaw, 1974), and 7.0 cm^3 accounts for the air volume under the cushion that is lateral to the concha, which we measured by filling the earphone cushion with water from a calibrated syringe.

[4]An ''effective'' middle-ear cavity compliance can be defined for conditions in which Z_{CAV} has an angle of approximately -0.25 cycles. Because of the effect of M_{ad}, the ''effective'' middle-ear compliance depends on frequency. At the lower frequencies where the effect of M_{ad} is negligible, the ''effective'' compliance is the total compliance C_t+C_a. For frequencies much greater than the parallel resonant frequency between the mass M_{ad} and the compliances C_a and C_t, the ''effective'' compliance is C_t [see the plot of Z_{CAV} in Fig. 5(B)]. In general, when $\angle Z_{\mathrm{CAV}}\approx -0.25$ (cycles), the ''effective'' compliance $C_{\mathrm{eff}}\approx 1/(\omega|Z_{\mathrm{CAV}}|)$ where $\omega=2\pi f$.

[5]Perforations that cover 1% and 4% of the tympanic-membrane area correspond to circular perforations with diameters of 1 mm and 2 mm, respectively, assuming a tympanic-membrane area of 70 mm^2, which is the median of the 55 mm^2 to 85 mm^2 range given by Wever and Lawrence (1954, p. 416).

[6]A possible complication might occur in the process of altering the impedance at the tympanic membrane Z_{TM} from its normal value to an infinite magnitude. We assume a process in which the impedance Z_{TM} varies such that $|Z_{TM}^{\mathrm{NORMAL}}|\leqslant|Z_{TM}|\leqslant\infty$ with the angle of Z_{TM} equal to the angle of Z_{TM}^{NORMAL}. To simplify our discussion here, we consider admittances, where for example, $Y_{TM}=1/Z_{TM}$, $Y_{EE}=1/Z_{EE}$, and $Y_{TH}=1/Z_{TH}$. For all cases represented by Fig. 9, $|Y_{NET}|=|Y_{TH}+Y_{EE}+Y_{TM}|$ decreases when $|Y_{TM}|$ decreases from $|Y_{TM}^{\mathrm{NORMAL}}|$ to zero, and therefore $|P_{EC}|$ increases. It is, however, conceivable that some values of Y_{TM} could occur which would produce an increase in $|Y_{NET}|$, when $|Y_{TM}|$ decreases. For instance, if $Y_{EE}=j\omega B_{EE}$ and $Y_{TM}^{\mathrm{NORMAL}}=-j\omega B_{EE}=-j\omega B_{TM}$, the sum $Y_{EE}+Y_{TM}$ would be zero and as $B_{TM}\rightarrow 0$, the sum would increase in magnitude. Because the imaginary part of Y_{TM} is generally positive (as is $B_{EE}=C_{EE}$), this effect will not occur for most conditions. For conditions (e.g., frequencies above 2000 Hz) where the imaginary part of Y_{TM} can be negative (see, e.g., Rosowski *et al.*, 1990, Fig. 10), the angles are rarely more positive than 1/8 of a period, so the resonance will not produce a sharp increase in $|Y_{NET}|$ and any deviation from a uniform decrease in $|Y_{NET}|$ will not be dramatic.

[7]A terminating impedance that represents a radiation impedance results in essentially the same tube impedance as the terminating impedance of zero.

[8]The model prediction was compared visually to the data with different model volumes until the model and data had similar magnitudes below 1000 Hz.

Allen, J. B. (**1986**). ''Measurement of eardrum acoustic impedance,'' in *Peripheral Auditory Mechanisms*, edited by J. B. Allen, J. L. Hall, A. Hubbard, S. T. Neely, and A. Tubis (Springer-Verlag, New York), pp. 44–51.

Berry, Q. C., Andrus, W. S., Bluestone, C. D., and Cantekin, E. I. (**1975**). ''Tympanometric pattern classification in relation to middle ear effusions,'' Ann Otol. **84**, 56–64.

Borton, T. E., Nolen, B. L., Luks, S. B., and Meline, N. C. (**1989**). ''Clinical applicability of insert earphones for audiometry,'' Audiology **28**, 61–70.

Bright, R. A., Moore, R. M., Jeng, L. L., Sharkness, C. M., Hamburger, S. E., and Hamilton, P. M. (**1993**). ''The prevalence of tympanostomy tubes in children in the United States, 1988,'' American Journal of Public Health **83**, 1026–1028.

Burkhard, M. D., and Corliss, E. L. R. (**1954**). ''The response of earphones in ears and couplers,'' J. Acoust. Soc. Am. **26**, 679–685.

Egolf, D. (**1977**). ''Mathematical modeling of a probe-tube microphone,'' J. Acoust. Soc. Am. **61**, 200–205.

Harris, J. D. (**1978**). ''Proem to a quantum leap in audiometric data collection and management,'' Heart Vessels Suppl. **18**, 1–29.

Keefe, D. H., Bulen, J. C., Arehart, K. H., and Burns, E. M. (**1993**). ''Ear-canal impedance and reflection coefficient in human infants and adults,'' J. Acoust. Soc. Am. **94**, 2617–2638.

Killion, M. C., and Villchur, E. (**1989**). ''Comments on ''Earphones in audiometry'' [Zwislocki *et al.*, J. Acoust. Soc. Am. **83**, 1688–1689 (1988)],'' J. Acoust. Soc. Am. **85**, 1775–1778.

Kringlebotn, M. (**1988**). ''Network model for the human middle ear,'' Scand. Audiol. **17**, 75–85.

Kruger, B., and Tonndorf, J. (**1977**). ''Middle ear transmission in cats with experimentally induced tympanic membrane perforations,'' J. Acoust. Soc. Am. **61**, 126–132.

Kruger, B., and Tonndorf, J. (**1978**). ''Tympanic membrane perforations in cats: Configurations of losses with and without ear canal extensions,'' J. Acoust. Soc. Am. **63**, 436–441.

Lim, D. (**1970**). ''Human tympanic membrane an ultrastructural observation,'' Acta Oto-Laryngol. **70**, 176–186.

Lynch, T. J., Peake, W. T., and Rosowski, J. J. (**1994**). ''Measurements of the acoustic input impedance of cat ears: 10 Hz to 20 kHz,'' J. Acoust. Soc. Am. **96**, 2184–2209.

Merchant, S. N. (**1997**). Personal communication.

Merchant, S. N. (**1999**). Personal communication.

Molvaer, O., Vallersnes, F., and Kringlebotn, M. (**1978**). ''The size of the middle ear and the mastoid air cell,'' Acta Oto-Laryngol. **85**, 24–32.

Morse, P. M., and Ingard, K. U. (**1968**). *Theoretical Acoustics* (McGraw-Hill, New York).

Nadol, Jr., J. B. (**1993**). ''Osseous Approaches to the Temporal Bone,'' *Surgery of the Ear and Temporal Bone*, edited by J. B. Nadol, Jr. and Harold F. Schuknecht (Raven Press, New York), Chap. 9, pp. 99–110.

Neely, S. T., and Gorga, M. P. (**1998**). ''Comparison between intensity and pressure as measures of sound level in the ear canal,'' J. Acoust. Soc. Am. **104**, 2925–2934.

Rabinowitz, W. M. (**1981**). ''Measurement of the acoustic input immittance of the human ear,'' J. Acoust. Soc. Am. **70**, 1025–1035.

Rosowski, J. J., Davis, P. J., Merchant, S. N., Donahue, K. M., and Coltrera, M. D. (**1990**). ''Cadaver middle ears as models for living ears: comparisons of middle ear input impedance,'' Ann. Otol. Rhinol. Laryngol. **99**, 403–412.

Sadé, J. (**1982**). ''Prologue,'' in *Proceedings of the Second International Conference of Cholesteatoma and Mastoid Surgery*, edited by J. Sadé (Kugler Publications, Amsterdam), p. 1.

Shaw, E. A. G. (**1966**). ''Earcanal pressure generated by circumaural and supraaural earphones,'' J. Acoust. Soc. Am. **39**, 471–479.

Shaw, E. A. G. (**1974**). ''The external ear,'' in *Handbook of Sensory Physiology*, edited by W. D. Keidel and W. D. Neff (Springer-Verlag, Berlin), Chap. 14, pp. 455–490.

Unge, M. von W. D., Dirckx, J., and Bagger-Sjöbäck, D. (**1995**). ''Shape and displacement patterns of the gerbil tympanic membrane in experimental otitis media with effusion,'' Hear. Res. **82**, 184–196.

Voss, S. E. (**1998**). ''Effects of tympanic-membrane perforations on middle-ear sound transmission: measurements, mechanisms, and models,'' Ph. D. thesis, MIT.

Voss, S. E., and Allen, J. B. (**1994**). ''Measurement of acoustic impedance and reflectance in the human ear canal,'' J. Acoust. Soc. Am. **95**, 372–384.

Voss, S. E., Rosowski, J. J., Merchant, S. N., Thornton, A. R., Shera, C. A., and Peake, W. T. (**in press**). ''Middle-ear pathology can affect the ear-canal sound pressure generated by audiologic earphones,'' Ear Hear. (in press).

Wever, E. G., and Lawrence, M. (**1954**). *Physiological Acoustics* (Princeton University Press, Princeton, NJ).

Wilber, L. A. (**1994**). ''Calibration, puretone, speech and noise signals,'' in *Handbook of Clinical Audiology*, edited by J. Katz (Williams & Wilkins, Baltimore, MD), Chap. 6, pp. 73–94.

Zwislocki, J. (**1962**). ''Analysis of the middle-ear function. Part 1: Input impedance,'' J. Acoust. Soc. Am. **34**, 1514–1523.

Zwislocki, J., and Feldman, A. (**1970**). ''Acoustic impedance in normal and pathological ears,'' American Speech and Hearing Association Monograph **15**, 1–42.

Zwislocki, J., Kruger, B., Miller, J. D., Niemoeller, A. F., Shaw, E. A., and Studebaker, G. (**1988**). ''Earphones in audiometry,'' J. Acoust. Soc. Am. **83**, 1688–1689.